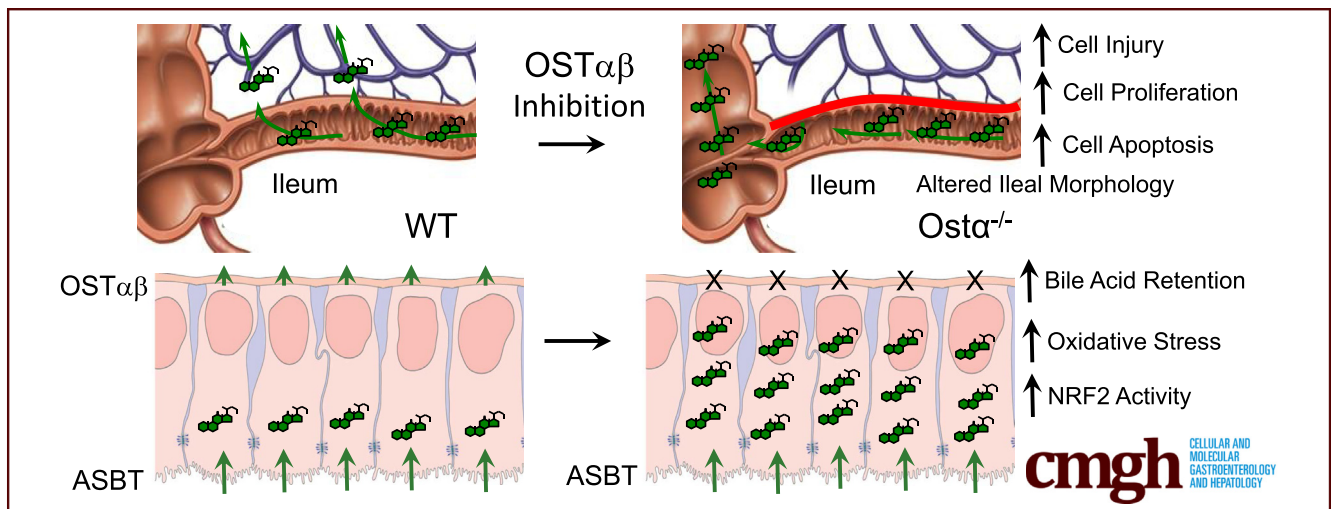


ORIGINAL RESEARCH

Organic Solute Transporter α - β Protects Ileal Enterocytes From Bile Acid–Induced Injury

Courtney B. Ferrebee,^{1,2} Jianing Li,¹ Jamie Haywood,² Kimberly Pachura,¹ Brian S. Robinson,³ Benjamin H. Hinrichs,³ Rheinallt M. Jones,¹ Anuradha Rao,¹ and Paul A. Dawson^{1,4}

¹Department of Pediatrics, Division of Gastroenterology, Hepatology, and Nutrition, ³Department of Pathology, Emory University, Atlanta, Georgia; ²Department of Internal Medicine, Wake Forest School of Medicine, Winston-Salem, North Carolina; ⁴Children's Healthcare of Atlanta, Atlanta, Georgia



SUMMARY

Enterocyte bile acid stasis in early postnatal life results in bile acid–induced cytotoxicity, oxidative stress, and a restitution response. Blocking enterocyte apical membrane bile acid uptake protects against ileal epithelial injury.

BACKGROUND & AIMS: Ileal bile acid absorption is mediated by uptake via the apical sodium-dependent bile acid transporter (ASBT), and export via the basolateral heteromeric organic solute transporter α - β (OST α -OST β). In this study, we investigated the cytotoxic effects of enterocyte bile acid stasis in *Ost α ^{-/-}* mice, including the temporal relationship between intestinal injury and initiation of the enterohepatic circulation of bile acids.

METHODS: Ileal tissue morphometry, histology, markers of cell proliferation, gene, and protein expression were analyzed in male and female wild-type and *Ost α ^{-/-}* mice at postnatal days 5, 10, 15, 20, and 30. *Ost α ^{-/-}Asbt^{-/-}* mice were generated and analyzed. Bile acid activation of intestinal Nrf2-activated pathways was investigated in *Drosophila*.

RESULTS: As early as day 5, *Ost α ^{-/-}* mice showed significantly increased ileal weight per length, decreased villus height, and increased epithelial cell proliferation. This correlated with premature expression of the *Asbt* and induction of bile

acid–activated farnesoid X receptor target genes in neonatal *Ost α ^{-/-}* mice. Expression of reduced nicotinamide adenine dinucleotide phosphate oxidase-1 and Nrf2–anti-oxidant responsive genes were increased significantly in neonatal *Ost α ^{-/-}* mice at these postnatal time points. Bile acids also activated Nrf2 in *Drosophila* enterocytes and enterocyte-specific knockdown of Nrf2 increased sensitivity of flies to bile acid–induced toxicity. Inactivation of the *Asbt* prevented the changes in ileal morphology and induction of anti-oxidant response genes in *Ost α ^{-/-}* mice.

CONCLUSIONS: Early in postnatal development, loss of *Ost α* leads to bile acid accumulation, oxidative stress, and a restitution response in ileum. In addition to its essential role in maintaining bile acid homeostasis, *Ost α* -*Ost β* functions to protect the ileal epithelium against bile acid–induced injury. NCBI Gene Expression Omnibus: GSE99579. (*Cell Mol Gastroenterol Hepatol* 2018;5:499–522; <https://doi.org/10.1016/j.jcmgh.2018.01.006>)

Keywords: Ileum; Reactive Oxygen Species; Nuclear Factor Erythroid-Derived 2-Like 2; Neonate; *Drosophila*.

In the hepatocyte, bile acids are synthesized from cholesterol, conjugated to taurine or glycine, and then secreted into bile for storage in the gallbladder or passage into the small intestine. During a meal, bile acids are present

in high concentration in the small intestine where they act as detergents to facilitate absorption of fats, fat-soluble vitamins, and cholesterol. After reaching the distal small intestine, bile acids are almost quantitatively reabsorbed by ileal enterocytes, and carried back to the liver in the portal circulation for uptake and resecretion into bile.¹ This enterohepatic circulation functions to safely store and then promptly deliver bile acids to the intestinal lumen, while limiting the systemic distribution and potential cytotoxicity of these amphipathic molecules. The major membrane carriers that maintain the enterohepatic circulation of bile acids are known and include specific transporters expressed on the sinusoidal and canalicular membranes of the hepatocyte, and on the apical brush border and basolateral membranes of the ileal enterocyte.² In ileum, the apical sodium-dependent bile acid transporter (ASBT) (gene symbol: *SLC10A2*) and the heteromeric organic solute transporter α - β (*OST α* -*OST β*) (gene symbols: *SLC51A*-*SLC51B*) mediate these steps, respectively.^{3,4} ASBT mutations in human beings or inactivation of the *Asbt* in mice yields a primary bile acid malabsorption phenotype that is characterized by impaired intestinal bile absorption, induction of hepatic bile acid synthesis, and increased fecal loss of bile acids in the absence of ileal histologic or ultrastructural changes.⁵⁻⁷ Inactivation of *Osta* in mice also impairs intestinal bile acid absorption. However, unlike *Asbt*^{-/-} mice or patients with ASBT mutations, *Osta*^{-/-} mice show a complex phenotype that includes a paradoxical reduction in hepatic bile acid synthesis and ileal hypertrophy.^{8,9} The changes in bile acid metabolism are associated with altered gut-liver bile acid signaling through the farnesoid X receptor (FXR)-fibroblast growth factor (FGF)15/19-FGF receptor 4 pathway, and inactivation of FXR in *Osta*^{-/-} mice reverses the reductions in hepatic *Cyp7a1* expression and bile acid synthesis.⁸⁻¹⁰ By contrast, the altered ileal morphology in *Osta*^{-/-} mice is not affected by inactivation of FXR.¹¹ The ileal changes observed in *Osta*^{-/-} mice, which include villous blunting, are typically associated with epithelial damage and subsequent healing.¹² Although adult *Osta*^{-/-} mice do not show overt symptoms of intestinal injury, such as increased inflammatory gene expression in ileum, bleeding, or diarrhea, newborn *Osta*^{-/-} mice show a small postnatal growth deficiency, and this may coincide with the onset of injury or initiation of an adaptive response.^{8,9}

The cause of the altered ileal morphology in *Osta*^{-/-} mice is unclear, but may involve bile acids. Conjugated bile acids are fully ionized at physiological pH and are largely membrane-impermeable in the absence of transporters. As such, conjugated bile acid accumulation and intracellular toxicity occurs when membrane transporters facilitate their uptake and their cellular export is inhibited.¹³ Bile acid-induced damage is best described for forms of liver disease and has been studied for hepatocytes and the biliary epithelium.^{14,15} For example, in progressive familial intrahepatic cholestasis type 2, inherited mutations in the bile salt export pump (gene symbol: *ABCB11*) blocks canalicular bile acid export, leading to the accumulation of bile acids and subsequent hepatocellular damage.¹⁶ The molecular mechanisms implicated in bile acid-induced


hepatocyte injury include induction of endoplasmic reticulum stress and mitochondrial damage.^{14,17-20} However, more recent studies have suggested that intracellular conjugated bile acids indirectly stimulate hepatocyte chemokine expression and induce liver injury via a hepatocyte-initiated inflammatory response.^{15,21} Beyond the liver and biliary tract, there is a substantial flux of bile acids across the ileal epithelium. Surprisingly little is known regarding how the ileal enterocyte is protected against bile acid cytotoxicity.²²⁻²⁴ In *Osta*^{-/-} mice, we hypothesize that continued ileal enterocyte ASBT-mediated bile acid uptake in the absence of a mechanism for efficient export will increase intracellular bile acid levels. This in turn can promote bile acid-induced injury and drive the apparent epithelial damage observed. The ontogeny of bile acid synthesis and transport has been carefully described in rats and mice, with an abrupt induction of ileal ASBT expression coinciding with concentrative bile acid uptake between postnatal days 17 and 21.²⁵⁻²⁸ If bile acids are important for the morphologic changes observed in *Osta*^{-/-} mice, then ASBT-mediated bile acid uptake into the ileal enterocytes should precede or coincide with the intestinal injury. To test this hypothesis, we investigated the temporal relationship in *Osta*^{-/-} mice between the intestinal adaptive response and initiation of active ileal bile acid absorption, and whether inactivation of the ASBT is protective in *Osta*^{-/-} mice. The potential mechanisms underlying the postulated bile acid-induced injury also were explored with a reductionist approach using the *Drosophila* model organism.

Materials and Methods

Animals, Treatments, and Tissue Collection

The Institutional Animal Care and Use Committees at the Wake Forest School of Medicine and Emory University approved these experiments. The *Osta*^{-/-} and *Asbt*^{-/-} mice were generated as previously described.^{7,8} The mice were backcrossed onto a C57BL/6J background for 8 generations and compared with wild-type (WT) littermates on the same background. The *Osta*^{-/-}*Asbt*^{-/-} mice were generated by cross-breeding the corresponding null mice and compared with lines generated from WT, *Osta*^{-/-}, and *Asbt*^{-/-} littermates as controls. The mice were group-housed in ventilated cages

Abbreviations used in this paper: ARE, anti-oxidant response element; Asbt, apical sodium-dependent bile acid transporter; CDCA, chenodeoxycholic acid; cRNA, complementary RNA; FGF, fibroblast growth factor; FXR, farnesoid X receptor; GAPDH, glyceraldehyde-3-phosphate dehydrogenase; GFP, green fluorescence protein; GSH, reduced glutathione; GSSG, oxidized glutathione; Ibabp, ileal bile acid binding protein; mRNA, messenger RNA; NEC, necrotizing enterocolitis; Nox, reduced nicotinamide adenine dinucleotide phosphate oxidase; Nrf2, nuclear factor (erythroid-derived 2)-like 2; Ost, organic solute transporter; PBS, phosphate-buffered saline; ROS, reactive oxygen species; TNF, tumor necrosis factor; TUNEL, terminal deoxynucleotidyl transferase-mediated deoxyuridine triphosphate nick-end labeling; WT, wild type.

 Most current article

© 2018 The Authors. Published by Elsevier Inc. on behalf of the AGA Institute. This is an open access article under the CC BY-NC-ND license (<http://creativecommons.org/licenses/by-nc-nd/4.0/>).

2352-345X

<https://doi.org/10.1016/j.jcmgh.2018.01.006>

(Super Mouse 750 Microisolator System; Lab Products, Seaford, DE) containing bedding (1/8" Bed-O-Cobbs; Andersons Lab Bedding Products, Maumee, OH) in the same temperature- (22°C) and light/dark cycle- (12-h; 6 AM to 6 PM) controlled room of the animal facility to minimize environmental differences. The breeding mice were maintained in cages with standard bedding (1/8" Bed-O-Cobbs) and pulp cotton fiber nesting material (Nestlets; Ancare, Bellmore, NY), fed ad libitum rodent breeder chow (21% of calories as fat; PicoLab Diet 20 no. 5058; catalog no. 0007689, LabDiet, St. Louis, MO), and offspring were weaned at postnatal day 20. The higher fat content breeder chow was fed to the dams because previous studies noted small postnatal growth deficits in *Ost α ^{-/-}* and *Asbt^{-/-}* mice.^{7,8} Adult nonbreeding mice were maintained on rodent chow (13% of calories as fat; PicoLab Diet 20 no. 5053, catalog no. 0007688, LabDiet). For the ontogeny study, WT and *Ost α ^{-/-}* breeders were closely monitored for pregnancy status. Offspring were collected within 4 hours of the end of the dark phase on postnatal days 5, 10, 15, 20, and 30. The sex of the pups at day 5 was confirmed by genotyping for the presence of the Y chromosome as described.²⁹ Body weight, small intestinal length, and segment wet weight were recorded at necropsy from 2 to 4 litters ($n \geq 7$ mice) per genotype and time point. For the ontogeny study, the small intestine was divided into 3 equal-length segments for histology and analysis of gene expression or 5 equal-length segments for bile acid analysis; segments were flushed with ice-cold phosphate-buffered saline (PBS) to remove luminal contents before weighing and analysis. For histologic analysis, the small intestinal segments were fixed for paraffin embedding. For measurements of bile acid content or gene and protein expression, the tissues were flash-frozen in liquid nitrogen and stored at -80°C before analysis. For analysis of the *Asbt*-*Ost α* double-null mice, male *Ost α ^{-/-}Asbt^{-/-}* and corresponding control mice were analyzed at 10 days and at 8–10 weeks of age. The adult mice were fasted for approximately 4 hours at the end of the dark phase before being euthanized to isolate tissues. For the adult *Ost α ^{-/-}Asbt^{-/-}* and control mice, the small intestine was subdivided into 5 equal-length segments and flushed with ice-cold PBS to remove luminal contents before being fixed for histologic analysis or flash-frozen in liquid nitrogen and stored at -80°C for measurements of gene expression.^{8,10}

Histologic and Immunohistochemical Analysis

The intestinal segments were flushed with PBS to remove luminal contents, fixed overnight in 10% neutral formalin (Sigma-Aldrich), and stored in 60% ethanol until processed for histology. Each segment was cut into longitudinal strips, stacked, and encased in 2% agarose before being embedded in paraffin and processed by Children's Healthcare of Atlanta Pathology Services. Histologic sections (5 μ m) were cut and stained with H&E or used for immunohistochemical or immunofluorescence analysis. Microscopy was performed at the Emory University Integrated Cellular Imaging Core. The average villus heights of the proximal and midintestinal segments were measured for *Ost α ^{-/-}* and WT mice at postnatal days 5, 10, 15, 20, and 30. At least 20 well-oriented,

full-length, villus units per segment per mouse were measured; quantitative analysis of the digitally acquired images was performed using ImageJ software (National Institutes of Health, Bethesda, MD).³⁰ Because of the aberrant morphology of the *Ost α ^{-/-}* mice, quantitative measurements of crypt height were not performed for distal (ileal) segment at postnatal days 5, 10, 15, 20, and 30.

For detection of phosphohistone H3, a marker of cell proliferation, paraffin-embedded ileal sections underwent a heat-induced epitope retrieval procedure and were stained using a rabbit anti-phosphohistone H3 (Ser10) primary antibody (catalog no. 9701S, lot 13; Cell Signaling Technology, Danvers, MA) and Alexa Fluor 488-conjugated goat anti-rabbit antibody (catalog no. A-11034, lot 1670152; Thermo Fisher Scientific, Waltham, MA). For detection of apoptosis, terminal deoxynucleotidyl transferase-mediated fluorescein-deoxyuridine triphosphate nick-end labeling was performed using an in situ Cell Death Detection kit (catalog no. 11684795910, lot 10711900; Sigma-Aldrich) as described by the manufacturer. At least 3 mice were included for each experimental group or condition, and 6–8 field views at a magnification of 20 \times were taken for each ileal segment and analyzed for both phosphohistone H3 and terminal deoxynucleotidyl transferase-mediated deoxyuridine triphosphate nick-end labeling (TUNEL)-positive cells. Because individual crypt-villus structures were difficult to discern for *Ost α ^{-/-}* mice owing to the altered morphology, comparisons were made using the number of phosphohistone H3 or TUNEL-positive cells counted per unit of intestinal length. For detection of mouse ileal bile acid binding protein (Ibapp) (*Fabp6*), paraffin-embedded ileal sections underwent a heat-induced epitope retrieval procedure and were stained using rabbit anti-fatty acid binding protein 6 primary antibody (catalog no. ab91184, lot GR245572-3; Abcam, Cambridge, MA) and Alexa Fluor 488-conjugated goat anti-rabbit antibody (catalog no. A-11034, lot 1670152; Thermo Fisher Scientific).

Bile Acid and Glutathione Measurements

Feces were collected from single-housed adult mice over a 72-hour period to measure the total bile acid content by enzymatic assay.⁷ To measure ileal tissue-associated bile acids, the small intestine was divided into 5 equal segments, flushed with PBS, flash-frozen, and ground under liquid nitrogen using a mortar and pestle. After addition of [¹⁴C]cholic acid (PerkinElmer Life Sciences, Boston, MA) to monitor bile acid recovery, aliquots of ileal tissue were extracted in ethanol and the bile acids were quantified by enzymatic assay as described.³¹ To measure ileal tissue-associated reduced and oxidized glutathione levels, the small intestine was divided into 5 equal segments, flushed with PBS, and ileum (segment 5) was used to isolate mucosal cells that were frozen and stored at -80°C. After thawing, the samples were extracted using perchloric acid and chemically modified for analysis of dansyl derivatives by high-performance liquid chromatography using a fluorescence detector (Children's Healthcare of Atlanta and Emory University's Pediatric Biomarkers Core, Atlanta, GA).^{32,33}

Microarray and Measurements of Messenger RNA Expression

Total RNA was extracted from frozen tissue using TRIzol reagent (Invitrogen, Carlsbad, CA). For microarray analyses, ileal total RNA samples were purified further using an RNeasy MinElute Cleanup Kit (74204; Qiagen, Hilden, Germany), followed by quality assessment using an Agilent 2100 bioanalyzer. Samples with RNA integrity number values > 8.0 were carried forward for complementary RNA (cRNA) synthesis and hybridization to GeneAtlas MG-430 PM Array Strips (Affymetrix, Santa Clara, CA) following the manufacturer's recommended protocol. Briefly, approximately 250 ng of purified total RNA was reverse-transcribed and biotin-labeled to produce biotinylated cRNA targets according to the standard Affymetrix GeneAtlas 3'-IVT Express labeling protocol (GeneAtlas 3' IVT Expression Kit User Manual, P/N 702833 revision 4; Affymetrix). After fragmentation, 6 μ g of biotinylated cRNA was hybridized for 16 hours at 45°C with the Affymetrix GeneAtlas Mouse MG-430 PM Array Strips. Strips were washed and stained using the GeneAtlas Fluidics Station according to standard Affymetrix operating procedures (GeneAtlas System User's Guide; P/N 08-0306 revision A January 2010; Affymetrix) and subsequently scanned using the GeneAtlas Imager system. Fluidics control, scan control, and data collection were performed using the GeneAtlas Instrument Control Software version 1.0.5.267 (Affymetrix). The raw data generated were normalized using the robust multi-array average method.³⁴ Ontology and pathway analysis was performed using the Database for Annotation,

Visualization and Integrated Discovery (DAVID).³⁵ All microarray analyses were performed by the Wake Forest School of Medicine Cancer Genomics Shared Resource Core (Winston-Salem, NC). Quantitative real-time polymerase chain reaction analysis was performed and messenger RNA (mRNA) expression levels were calculated based on the delta-delta threshold cycle method; values are means of triplicate determinations and expression was normalized using cyclophilin.⁸ The primer sequences are provided in Table 1.

Measurements of Protein Expression

Small intestinal extracts were prepared, subjected to sodium dodecyl sulfate–polyacrylamide gel electrophoresis using a 4%–20% gradient (Tris-Glycine Midi Gel; Invitrogen), and analyzed by immunoblotting.⁸ Blots were stripped before re-probing with antibodies to the different bile acid transport proteins or re-probing with antibody to glyceraldehyde-3-phosphate dehydrogenase (GAPDH) to normalize for protein load. Protein expression was quantified by densitometry using a Microtek (Hsinchu, Taiwan) ScanMaker i900 and FujiFilm (Tokyo, Japan) Multiguage 3 software, and expression data were normalized to levels of the GAPDH loading control. Sources of the antibodies used in the study were as follows: anti-mouse Asbt,⁷ anti-mouse Ost α and anti-mouse Ost β ,⁸ anti-mouse Ibabp (anti-fatty acid binding protein 6, catalog no. ab91184, lot GR245572-3; Abcam), anti-GAPDH (catalog no. MA5-15738; Thermo Fisher Scientific), horseradish-peroxidase–conjugated goat anti-rabbit antibody (catalog no. A9169, lot 015M48581; Sigma-Aldrich),

Table 1. List of Primer Sequences Used for Real-Time PCR Analysis

Gene	Forward primer	Reverse primer
<i>Asbt</i>	5' TGGGTTTCTTCTGCTAGACT 3'	5' TGTTCTGCATTCCAGTTTCCAA 3'
<i>Cyclophilin</i>	5' TTCTTCATAACCACAGTCAAGACC 3'	5' TCCACCTCCGTACCACATC 3'
<i>Cyp7a1</i>	5' AGCAACTAAACAACCTGCCAGTACTA 3'	5' GTCCGGATATTCAAGGATGCA 3'
<i>Cyp8b1</i>	5' GCCTTCAAGTATGATCGGTTCT 3'	5' GATCTTCTTGCCCGACTTGTAGA 3'
<i>Diet1</i>	5' CACTCCAATGGGATTGATGA 3'	5' CGAAGTCCCAGGTAAGGAGA 3'
<i>FGF15</i>	5' GAGGACCAAAACGAACGAAATT 3'	5' ACGTCCTTGATGGCAATCG 3'
<i>GSTa1</i>	5' GGCAGAATGGAGTGCATCA 3'	5' TCCAAATCTTCCGGACTCTG 3'
<i>GSTa3</i>	5' AGGGAACAGCTTTTTTAACAAGAAA 3'	5' CCATCAAAGTAATGAAGGACTGG 3'
<i>GSTa4</i>	5' CCCCTGTAAGTGTCCGACTTC 3'	5' GGAATGTTGCTGATTCTTGCTT 3'
<i>GSTmu1</i>	5' GCAGCTCATCATGCTCTGTT 3'	5' CATTCTCAGGGATGGTCTTC 3'
<i>GSTmu3</i>	5' CCCGCATACAGCTCATGATA 3'	5' TTGCCAGGAAGTCCAGAGTAG 3'
<i>Ibabp</i>	5' CAAGGCTACCGTGAAGATGGA 3'	5' CCCACGACCTCCGAAGTCT 3'
<i>I11b</i>	5' TGTAATGAAAGACGGCACACC 3'	5' TCTTCTTTGGGTATTGCTTGG 3'
<i>Nox1</i>	5' CGCTCCCAGCAGAAGGTCGTGATTACCAAGG 3'	5' GGAGTGACCCCAATCCCTGCCCAACCA 3'
<i>Nqo1</i>	5' AGCGTTCGGTATTACGATCC 3'	5' AGTACAATCAGGGCTCTTCTCG 3'
<i>Nrf2</i>	5' CATGATGGACTTGGAGTTGC 3'	5' CCTCAAAGGATGTCAATCAA 3'
<i>OSTα</i>	5' TACAAGAACACCCCTTTGCC 3'	5' CGAGGAATCCAGAGACCAAA 3'
<i>OSTβ</i>	5' GTATTTTCGTGCAGAAGATGCG 3'	5' TTTCTGTTTGCCAGGATGCTC 3'
<i>SHP</i>	5' CGATCCTCTTCAACCCAGAT 3'	5' AGCCTCCTGTTGCAGGTGT 3'
<i>Slc13a1</i>	5' AATACGCGCTACCCTGATTG 3'	5' TTGGTTTTGCCACACTTGAA 3'
<i>TNFα</i>	5' TCTTCTCATTCTGCTTGTGG 3'	5' GGTCTGGGCCATAGAAGTGA 3'

GST, glutathione-S-transferase.

and horseradish-peroxidase-conjugated goat anti-mouse antibody (catalog no. sc-2005, lot K1915; Santa Cruz Biotechnology, Dallas, TX).

Drosophila Bile Acid Resistance and Staining Assays

The WT and indicated *Drosophila* lines were obtained from previously described sources and maintained on standard media at 25°C.³⁶ Unless otherwise indicated, the WT strain *w1118* was used for all assays. Whole-animal cytoprotection in *Drosophila* was measured in response to dietary bile acids. Groups of 30–50 adult WT *Drosophila* (age, 5 days) were starved for 3 hours and then transferred to a vial containing a 2 × 2 cm piece of Whatman filter paper (Sigma-Aldrich) soaked with a solution of 5% sucrose containing the indicated concentration of bile acid. Survivors were scored for up to 7 days or until 100% lethality. The percentage of surviving flies were recorded and compared by log-rank Mantel-Cox test. For detection of nuclear factor (erythroid-derived 2)-like 2 (Nrf2)/anti-oxidant response element (ARE)-dependent green fluorescent protein (GFP) expression, 5-day adult *gstD1-gfp* *Drosophila* were transferred to vials containing 5% sucrose plus 25 mmol/L chenodeoxycholate (CDCA) or to vials containing 5% sucrose plus 25 mmol/L *N,N'*-dimethyl-4,4'-bipyridinium dichloride (Paraquat) as a positive control to induce oxidative stress. After 30 minutes, the intestinal tract was removed, fixed in 4% paraformaldehyde, and fluorescence was detected by confocal microscopy. For detection of reactive oxygen species (ROS) generation, 5-day adult WT flies were transferred to vials containing 5% sucrose or 5% sucrose plus 25 mmol/L CDCA. After 12 hours, the intestinal tract was removed and incubated with 100 μ mol/L ROSstar 550 hydrocyanine ROS-sensitive reagent (catalog no. PN926-20000; LI-COR, Lincoln, NE) in Schneider's *Drosophila* media at room temperature. The intestine then was washed, fixed in 4% paraformaldehyde, and the fluorescence was visualized by confocal microscopy.^{37,38} Representative fluorescent images of 4 independent measurements are shown.

Statistical Analyses

Mean values \pm SEM are shown unless otherwise indicated. The data were evaluated for statistically significant differences using the Mann-Whitney test, the 2-tailed Student *t* test, or by analysis of variance (Tukey-Kramer honestly significant difference) (GraphPad Prism; Mountain View, CA). Differences were considered statistically significant at $P < .05$.

Access to the Data

All authors had access to the study data and reviewed and approved the final manuscript.

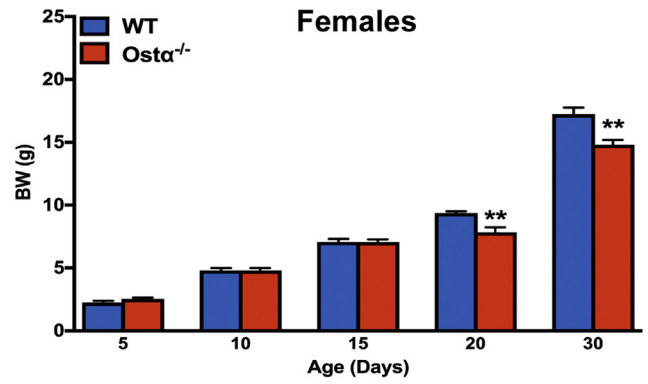
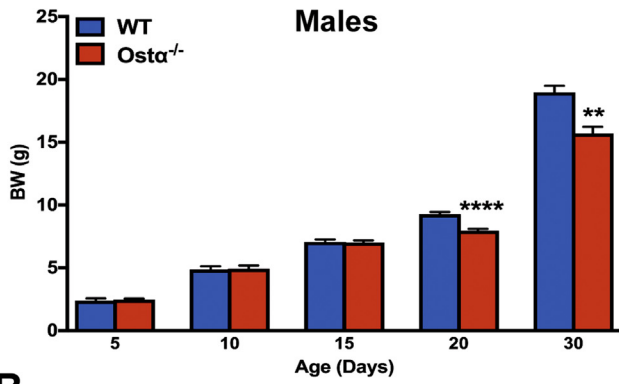
Results

Ontogeny of the Morphologic Changes in Small Intestine

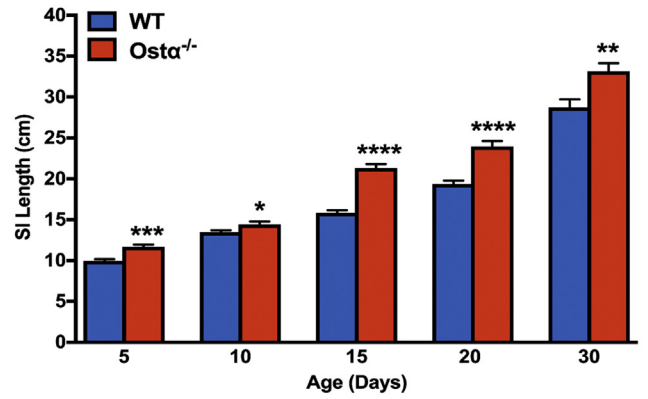
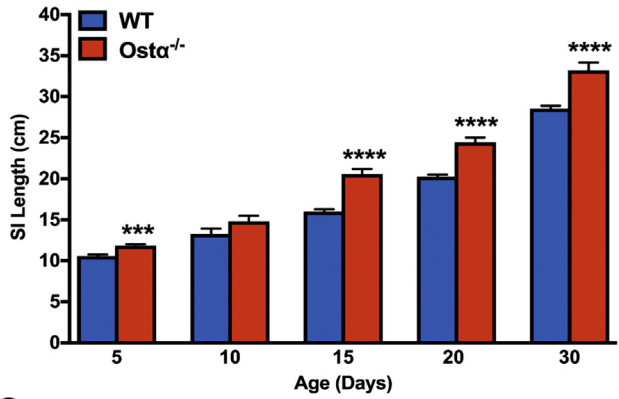
As previously reported,^{8–10} Ost α ^{-/-} mice backcrossed onto the C57BL/6J background are viable, fertile, and similar to

WT littermates in terms of survival and gross appearance. The body weights of male or female Ost α ^{-/-} mice were similar to WT mice at days 5, 10, and 15, but reduced at days 20 and 30 (Figure 1A). Small intestinal length and weight were increased as early as day 5 in male and female Ost α ^{-/-} mice compared with WT mice, and remained increased at days 10, 15, 20, and 30 (Figure 1B and C). The increase in mass per unit length was particularly evident for the distal small intestine (ileum) (Figure 1D). Analysis of the tissue morphology and histology showed little change in the proximal (duodenum) or midintestinal (jejunum) regions (data not shown). The villus heights were similar between WT and Ost α ^{-/-} mice in the proximal and midintestinal segments at postnatal days 5–15, with evidence of potential compensatory increases in villus height in jejunum at days 20 and 30 (Figure 2). In contrast, the ileal morphology and histology were altered dramatically in Ost α ^{-/-} mice (Figure 3). Compared with WT mice, the distal small intestine of Ost α ^{-/-} mice showed evidence of mucosal injury with features of regeneration. Specifically, Ost α ^{-/-} mice showed villous blunting that ranged from mild to severe, which was prominent at early ages of postnatal development (days 5, 10, and 15). The epithelium lining the villi showed regenerative changes including cellular pseudostratification and loss of nuclear polarity, particularly within the transit-amplifying zone and crypt neck (Figure 3B). In addition, the epithelium on the tips of villi in Ost α ^{-/-} mice showed altered apical borders and mucin synthesis. Although the tips of villi of WT mice are lined by absorptive enterocytes with an intact brush border and occasional mucin-producing goblet cells, the villous tips of Ost α ^{-/-} mice showed loss of the brush border and replacement by markedly increased numbers of mucin-secreting cells (Figure 3B). Consistent with increased rates of cell turnover, numerous apoptotic epithelial cells also were present near the villous tips as well as in the crypt regions. The lamina propria of Ost α ^{-/-} mice also contained mildly increased numbers of lymphocytes and macrophages with occasional neutrophils, eosinophils, and plasma cells. To confirm the histologic impression of increased crypt mitotic rate and the number of apoptotic cells in the ileum of Ost α ^{-/-} mice, cell proliferation and apoptosis were assessed using phosphohistone H3 and TUNEL staining, respectively. As early as postnatal day 5, there was an increase in the numbers of proliferating (phosphohistone H3-positive) cells in ileum of Ost α ^{-/-} compared with WT mice (Figure 4), consistent with the increased number of mitotic bodies noted in the histopathology assessment. There was also a trend toward an increased number of TUNEL-positive nuclei in the ileal villus structures of Ost α ^{-/-} vs WT mice (Figure 4). In agreement with the histologic absence of an active inflammatory response, the mRNA expression for proinflammatory genes tumor necrosis factor α (TNF α) and interleukin 1 β was not increased consistently in the ileal tissue of Ost α ^{-/-} mice (Figure 5). There was a trend toward higher expression of TNF α at early postnatal time points, with a significant increase at day 10 in males, but this was followed by significant reductions. In contrast to the markedly altered ileal tissue morphology, the liver weights and liver histology were similar in male and female WT and Ost α ^{-/-} at postnatal days

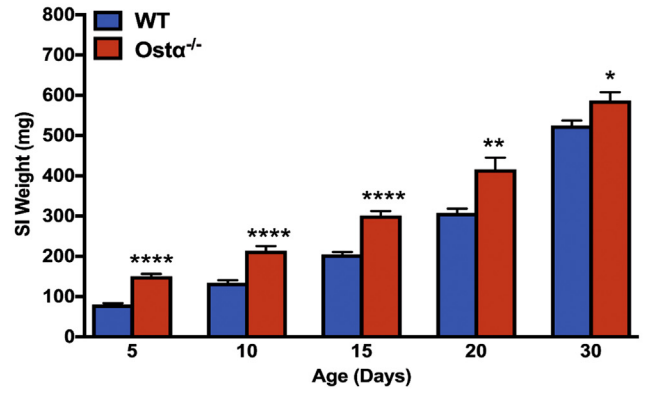
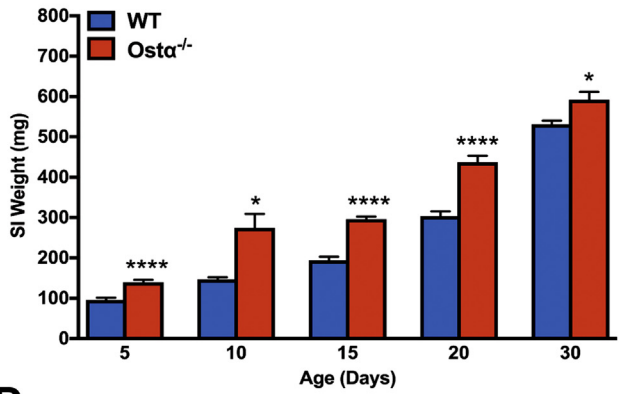
A



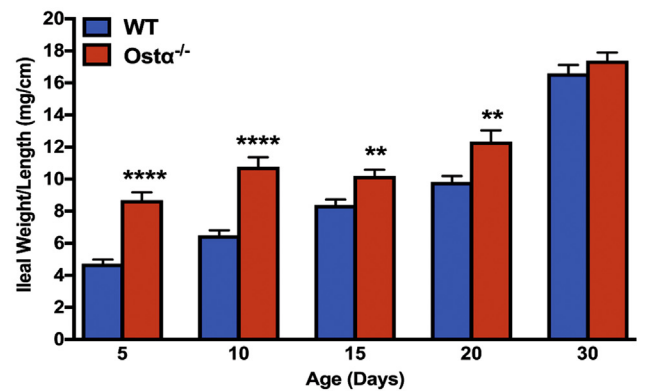
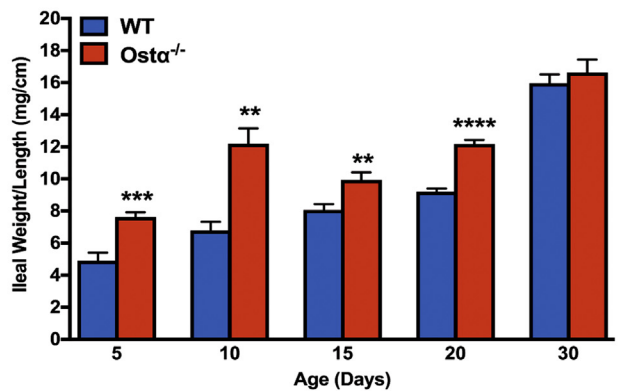
B



C



D



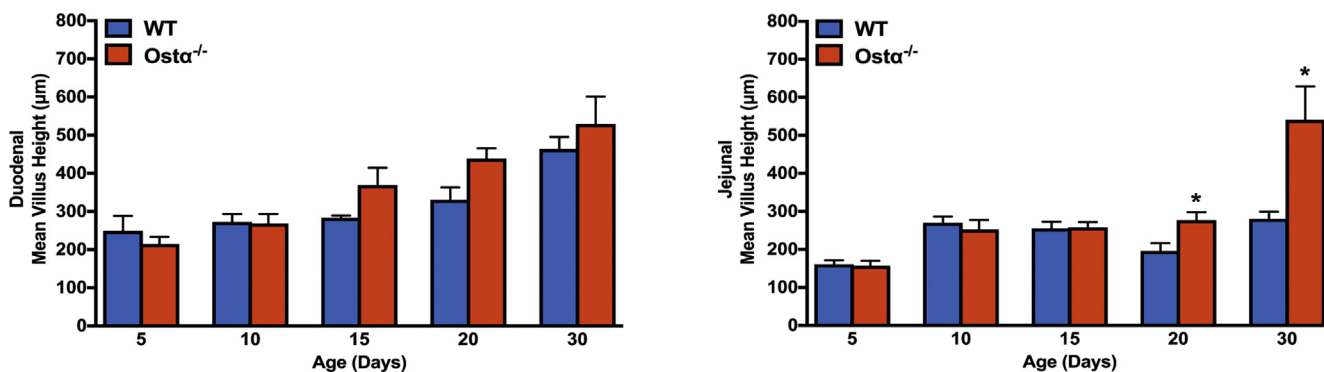


Figure 2. Intestinal morphology of proximal small intestine and jejunum in male and female WT and Ost $\alpha^{-/-}$ mice. Quantitative morphometric analysis of small intestine of WT and Ost $\alpha^{-/-}$ mice. The small intestine of mice of the indicated age and genotype was divided into 3 equal segments. H&E-stained sections from segments 1 and 2 were used to measure the villus height in 20 well-oriented, high-power fields per mouse. Data are expressed as the means ($n = 3-5$ mice per group). Mean values \pm SEM are shown. Significant differences between genotypes for that age were as follows: * $P < .05$.

5, 10, 15, 20, and 30 (data not shown), in agreement with previous studies of adult Ost $\alpha^{-/-}$ mice.^{39,40}

Expression of Bile Acid Transporters and FXR Target Genes in Distal Small Intestine

The intestinal morphologic changes in Ost $\alpha^{-/-}$ mice are evident before the normal induction of ileal concentrative bile acid uptake, which occurs between postnatal days 17 and 21 in WT mice.^{26,41} To determine if this temporal relationship is altered in Ost $\alpha^{-/-}$ mice, ileal bile acid transporter expression was examined in male (Figure 6) and female (Figure 7) WT and Ost $\alpha^{-/-}$ mice. In WT male and female mice, the mRNA and protein for Ost α -Ost β were expressed abundantly in distal small intestine at postnatal day 5, and increased 3- to 5-fold by day 20. In Ost $\alpha^{-/-}$ mice, mRNA and protein for the Ost α subunit were undetectable (Figures 6A and 7A). For the Ost β subunit (Figures 6B and 7B), the mRNA expression was increased in Ost $\alpha^{-/-}$ mice, but levels of Ost β protein were reduced in the absence of its partner protein Ost α , as previously reported.^{8,9,42} In WT mice, ileal Asbt mRNA and protein were almost undetectable at postnatal days 5 and 10, and their levels dramatically increased between postnatal days 15 and 20. By contrast, Asbt was expressed prematurely in Ost $\alpha^{-/-}$ mice, with ileal mRNA levels increased 12- to 28-fold in days 5 and 10 male and female Ost $\alpha^{-/-}$ as compared with WT mice (Figures 6C and 7C). This is associated with increased Asbt protein expression. After day 15, ileal Asbt mRNA and protein levels were lower in Ost $\alpha^{-/-}$ vs WT mice, in agreement with previous findings that ileal Asbt expression is reduced in adult (age, >8 wk) Ost $\alpha^{-/-}$ mice.¹⁰ An increase in Asbt expression in the absence of Ost α -Ost β -mediated bile acid export is predicted to increase the intracellular burden of bile acids in ileal

enterocytes and increase expression of target genes for the bile acid-activated nuclear receptor FXR. Consistent with an increased intracellular bile acid load, expression of the FXR target genes Ost β (Figures 6B and 7B), the cytosolic bile acid binding protein Ibabp (*Fabp6*) (Figures 6D and 7D), Shp (*Nr0b2*) (Figures 6E and 7E), and the sodium-sulfate cotransporter (*Slc13a1*) (Figures 6F and 7F) were induced in male and female Ost $\alpha^{-/-}$ as compared with WT mice at postnatal days 5-15. This was particularly evident for Ibabp, whose mRNA and protein levels were increased more than 100-fold at postnatal days 5 and 10. By immunofluorescence, Ibabp protein was readily detected in ileal enterocytes of Ost $\alpha^{-/-}$, but not WT mice at postnatal days 10 and 15 (Figure 6G). In agreement with the increased expression of FXR target genes, the ileal tissue bile acid content also was increased in 10-day-old Ost $\alpha^{-/-}$ vs WT mice (Figure 6H).

Molecular Mechanisms

Cellular accumulation of bile acids is associated with injury in a variety of diseases or disorders. The cytotoxic effects of bile acids have been attributed to several molecular mechanisms, including detergent-associated membrane damage, disruption of mitochondrial membrane potential, enhanced generation of ROS, direct activation of cell death receptors such as CD95/Fas and TNF-related apoptosis-inducing ligand receptor 2, and induction of an inflammatory response.^{15,22,43,44} To determine if similar mechanisms may be engaged in Ost $\alpha^{-/-}$ mice, microarray analysis of ileal gene expression was performed for adult male WT and Ost $\alpha^{-/-}$ mice at approximately 56 days of age (GEO series accession number: GSE99579). This analysis identified 244 differentially expressed genes (regulated more than 2-fold,

Figure 1. (See previous page). Ontogeny of the small intestinal morphologic changes in male and female WT and Ost $\alpha^{-/-}$ mice. (A) Body weight (BW). (B) Small intestinal (SI) length. (C) Small intestinal weight. (D) Distal small intestinal weight per unit length. The small intestine was subdivided into 3 equal-length segments and the weight of the distal third encompassing the ileum is shown as mg/cm length. Mice from 2 to 4 litters were included in the analysis for each sex, genotype, and postnatal age group ($n = 8-20$ per group). Mean values \pm SEM are shown. Significant differences between genotypes for that sex and age were as follows: * $P < .05$, ** $P < 0.01$, *** $P < .001$, and **** $P < .0001$.

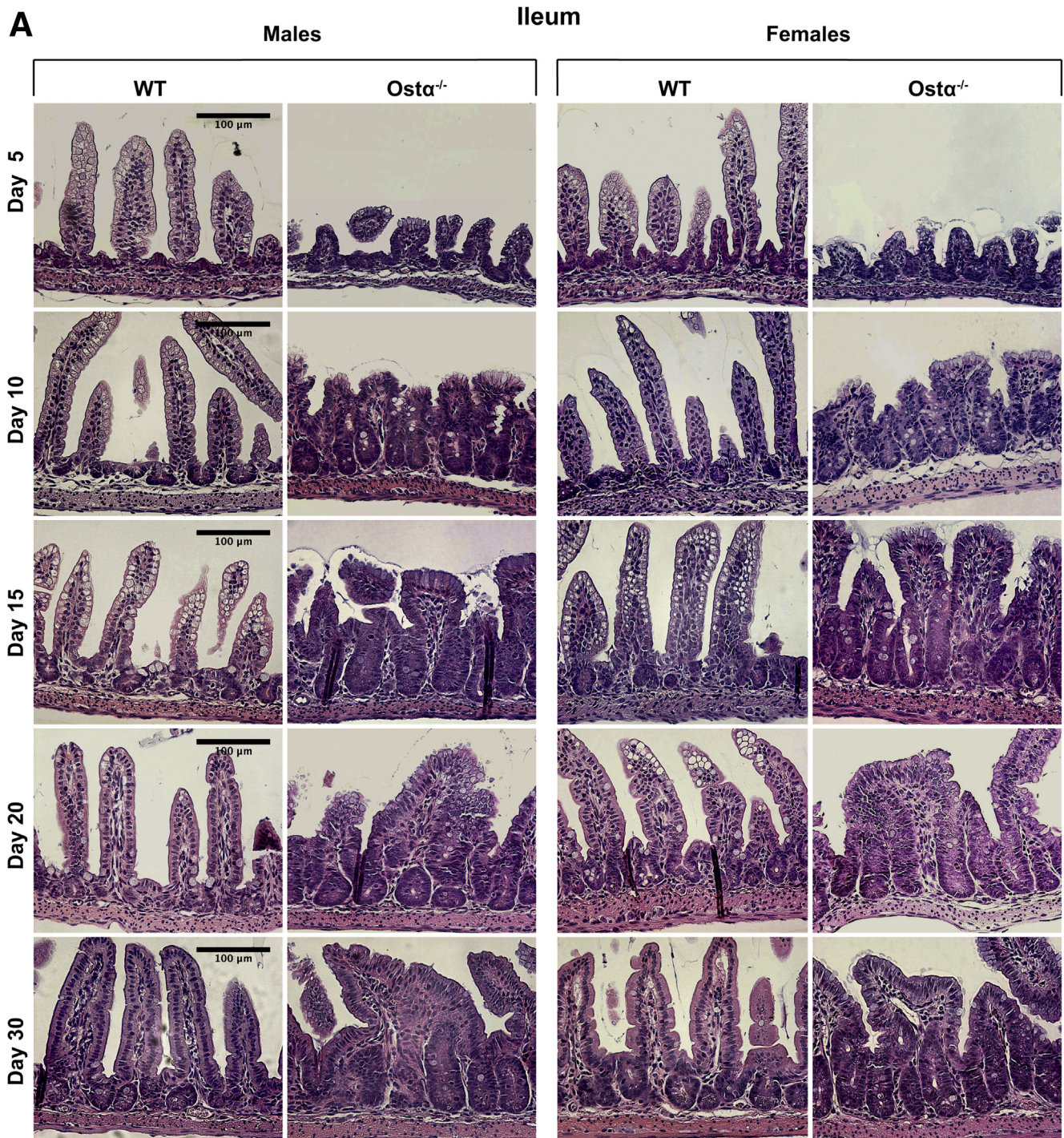


Figure 3. Ontogeny of the morphologic and histologic changes in the distal small intestine of male and female WT and *Osta*^{-/-} mice. (A) Representative light micrographs of H&E-stained transverse sections of distal small intestine. Original magnification, 20 \times . Scale bar: 100 μ m. (B) Representative light micrographs of H&E-stained transverse sections of distal small intestine from 10- and 15-day old WT and *Osta*^{-/-} mice. Original magnification, 40 \times . Scale bar: 50 μ m. The altered apical border and mucin-producing goblet cells at the villus tips of *Osta*^{-/-} mice are indicated by the *black arrows*. Mitotic figures, apoptotic cells, and immune cells in the *Osta*^{-/-} mice are indicated by the *white arrows*.

$P < .05$); the list included 54 and 190 genes that were increased and decreased, respectively. The induced genes are shown in the heat map in [Figure 8A](#). Ontogeny analysis performed for differentially expressed genes showed that

inactivation of *Osta* induced ileal gene expression for pathways related to oxidation-reduction, cell proliferation, and glutathione metabolism. In particular, there was increased expression of oxidant-responsive genes, with

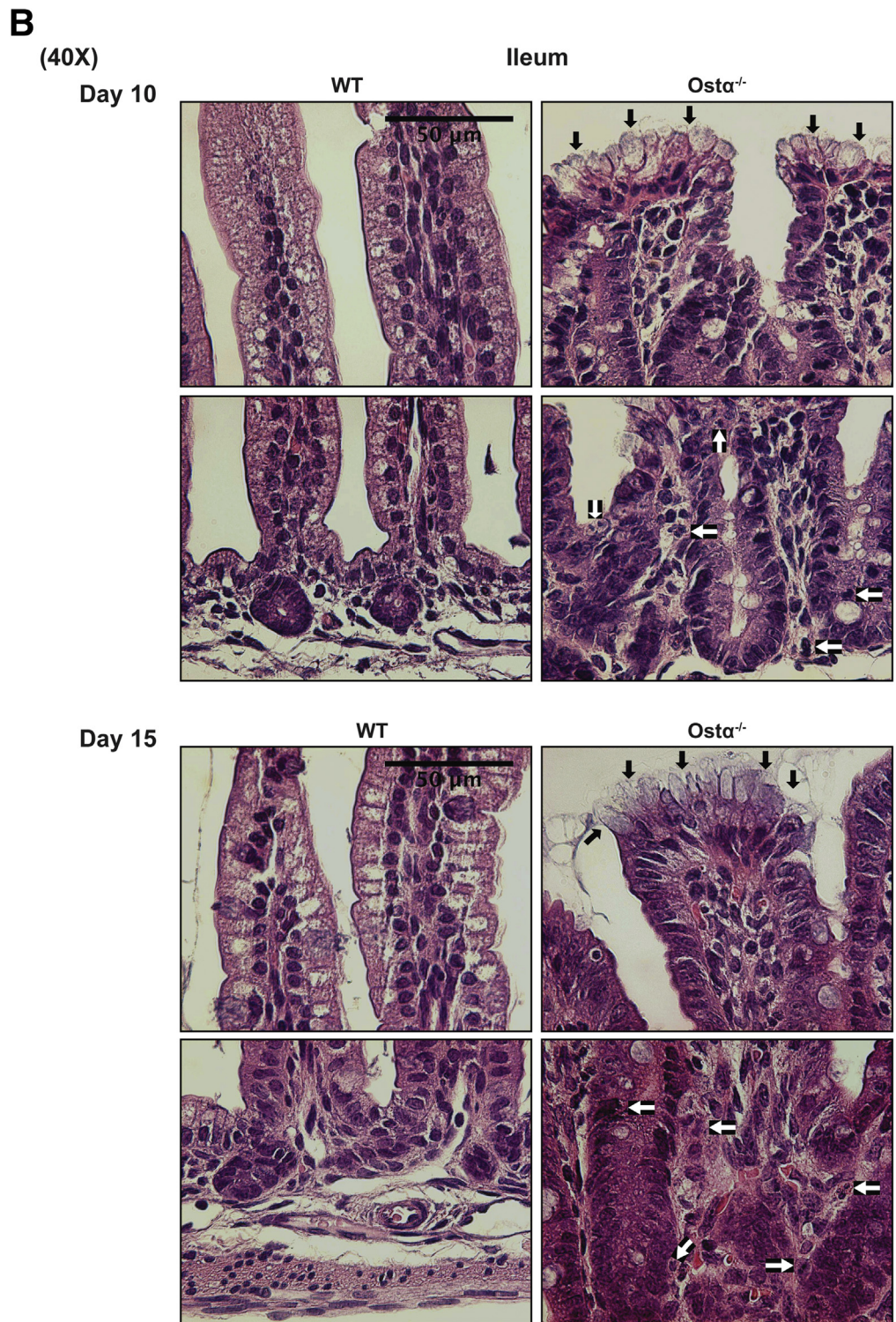


Figure 3. (continued)

Nrf2/ARE target genes among the most highly induced. The Nrf2 system responds to oxidative stress and is a major regulator of cytoprotective pathways.⁴⁵ In addition to the glutathione-S-transferase genes, Nrf2/ARE target genes induced in *Osta*^{-/-} mice included those involved in glutathione biosynthesis, such as glutamate-cysteine ligase catalytic subunit (increased 1.7-fold), glutamate-cysteine ligase

modifier (increased 1.4-fold), and glutathione synthetase (increased 1.6-fold), and those involved in glutathione metabolism, such as glutathione reductase (increased 2.2-fold) and glutathione peroxidase 2 (increased 1.5-fold). To determine how these gene expression changes may relate to the ileal glutathione redox status, the levels of reduced glutathione (GSH) and oxidized glutathione (GSSG) were

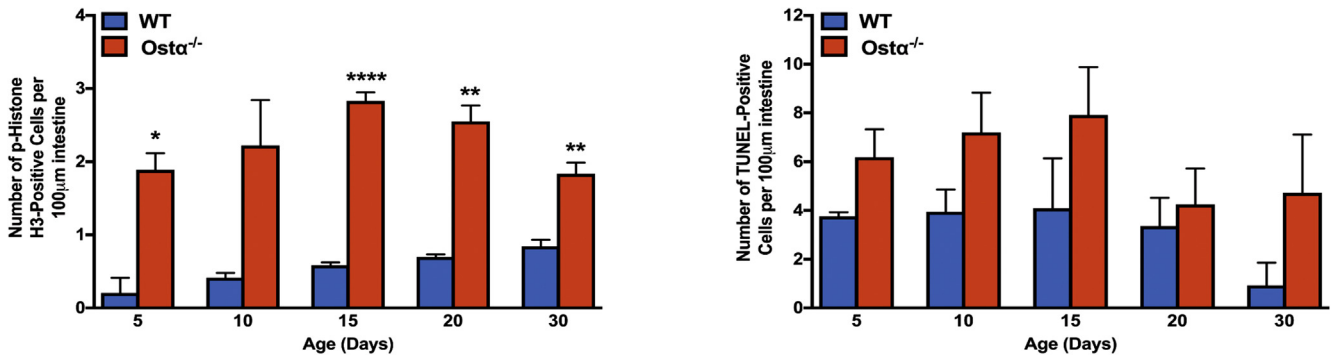


Figure 4. Ileal proliferation and apoptosis. Quantitation of the number of phosphohistone H3 and TUNEL-positive cells per unit area. Mice from 2 to 4 litters were included in the analysis for each genotype and postnatal age group ($n = 5-8$ per group). Mean values \pm SEM are shown. Significant differences between genotypes for that age were as follows: * $P < .05$, ** $P < .01$, and **** $P < .001$.

measured in ileal mucosa from adult *Osta*^{-/-} and WT mice ($n = 4$ /group). GSH levels (means \pm SEM, 2.09 ± 0.99 vs 6.34 ± 1.06 nmol/mg protein; $P < .05$) and the GSH-to-GSSG ratio (2.8 ± 1.2 vs 11.6 ± 3.0 ; $P < .05$), but not levels of GSSG (1.02 ± 0.27 vs 0.62 ± 0.10 nmol/mg protein; $P = .22$) were reduced significantly in the ileal mucosa of *Osta*^{-/-} vs WT mice, respectively.

To determine if there are similar gene expression changes in the neonatal mice, mRNA expression of the Nrf2

target genes *Gsta1*, *Gsta4*, and *Nqo1* was measured in male and female WT and *Osta*^{-/-} mice (Figure 8B). Consistent with the microarray analysis, expression of these genes was induced significantly in *Osta*^{-/-} mice vs WT mice as early as postnatal day 5. Because the ROS-generating enzyme reduced nicotinamide adenine dinucleotide phosphate oxidase 1 (Nox1) is expressed by the ileal epithelium and potentially involved in the redox-signaling associated with epithelial repair,^{38,46-48} Nox1 mRNA expression also was

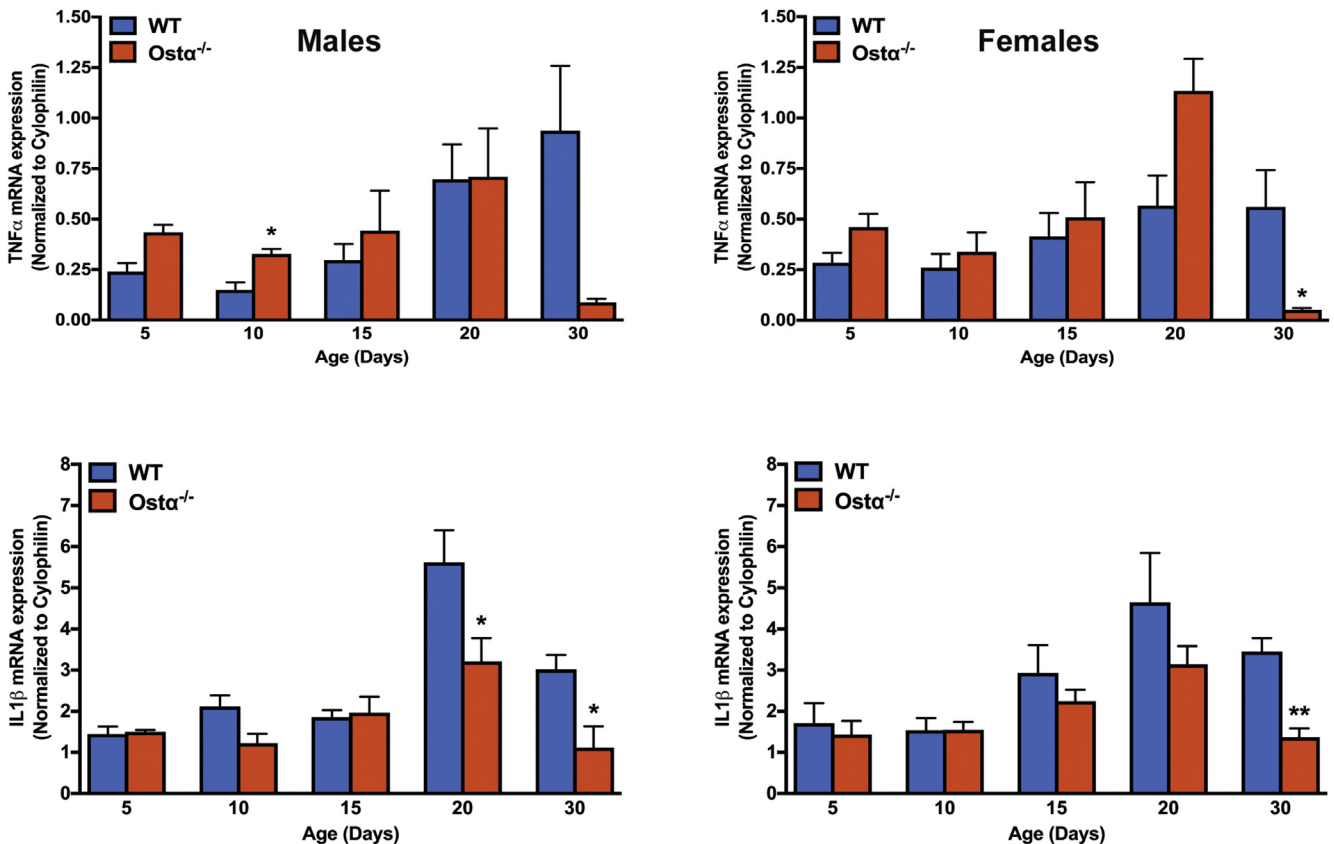


Figure 5. Expression of proinflammatory genes in ileum of male and female WT and *Osta*^{-/-} mice. RNA was isolated from the distal small intestine of individual mice ($n = 4-5$ per group) and used for real-time PCR analysis. The mRNA expression was normalized using cyclophilin. Mean values \pm SEM are shown. Significant differences between genotypes for that age and sex were as follows: * $P < .05$, ** $P < 0.01$.

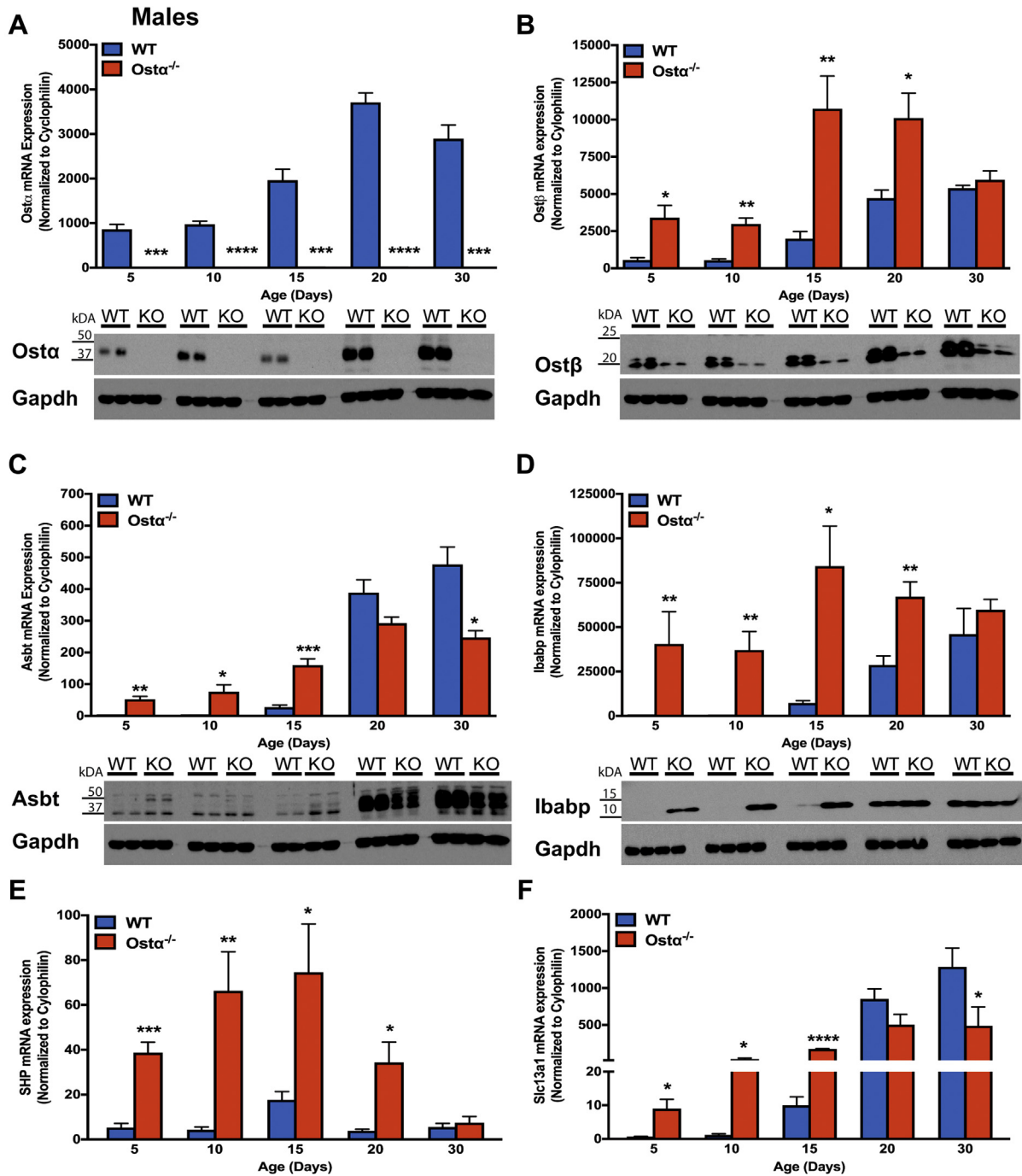


Figure 6. Expression of bile acid transporters and FXR target genes in distal small intestine of male WT and *Ost $\alpha^{-/-}$* mice. Expression of mRNA and protein for bile acid transport-related genes: (A) *Ost α* , (B) *Ost β* , (C) *Asbt*, and (D) *Ibabp*. Expression of mRNA for FXR target genes: (E) *Shp* and (F) *Slc13a1*. For mRNA expression measurements, RNA was isolated from the distal small intestine of individual male mice (n = 4–5 per group) and used for real-time PCR analysis. The mRNA expression was normalized using cyclophilin. For protein expression, extracts were prepared from distal intestine from individual male mice. Equal amounts of protein from 3 to 5 mice per group were pooled and duplicate samples were subjected to immunoblotting analysis. Blots were stripped and re-probed using antibodies to GAPDH as a loading control. (G) Immunostaining of transverse sections of distal small intestine for Ibabp. Original magnification: 20 \times . Scale bar: 100 μ m. (H) Ileal bile acid content of day 10 male WT and *Ost $\alpha^{-/-}$* mice. Bile acids were extracted from terminal ileum (last 20% of the small intestine) of 10-day-old male WT or *Ost $\alpha^{-/-}$* mice and quantified by enzymatic assay. The bile acid content is expressed as mass per whole ileum, mass per unit length of ileum, and mass per unit weight of ileum. For mRNA expression, bars indicate means \pm SEM. Significant differences between genotypes for that age were as follows: **P* < .05, ***P* < .01, and ****P* < .001, *****P* < .0001.

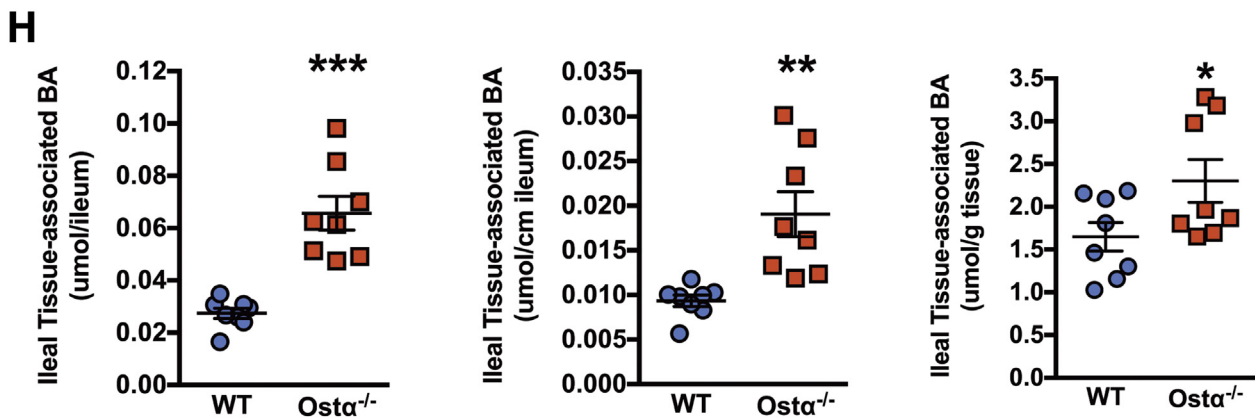
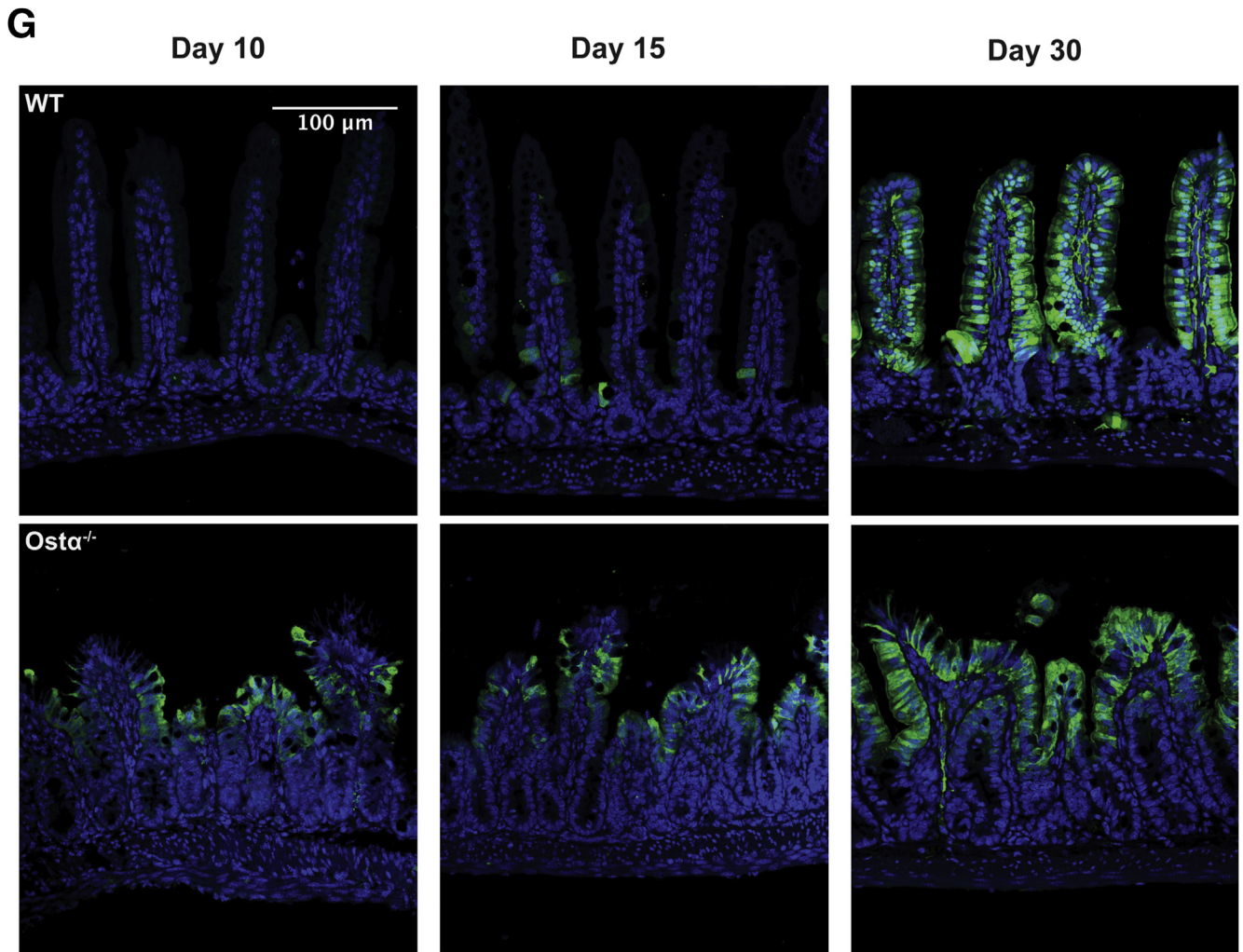


Figure 6. (continued)

measured and shown to be increased significantly in neonatal *Osta*^{-/-} mice (Figure 8C).

Nrf2 Protects Against Bile Acid Cytotoxicity

The results suggest that bile acids are inducing oxidative injury that is countered by expression of Nrf2-regulated cytoprotective genes. The findings are in agreement with a

prior in vitro study in Caco-2 cells that showed bile acids such as deoxycholic acid and lithocholic acid induced Nrf2-ARE target gene expression and Nrf2-knockdown cells were more susceptible to lithocholic acid-induced toxicity.⁴⁹ To directly test if intestinal Nrf2 is protective against bile acid-induced cytotoxicity in vivo, the model organism *Drosophila* was used. Components of the Nrf2 signaling pathway are conserved and fully developed in *Drosophila*,

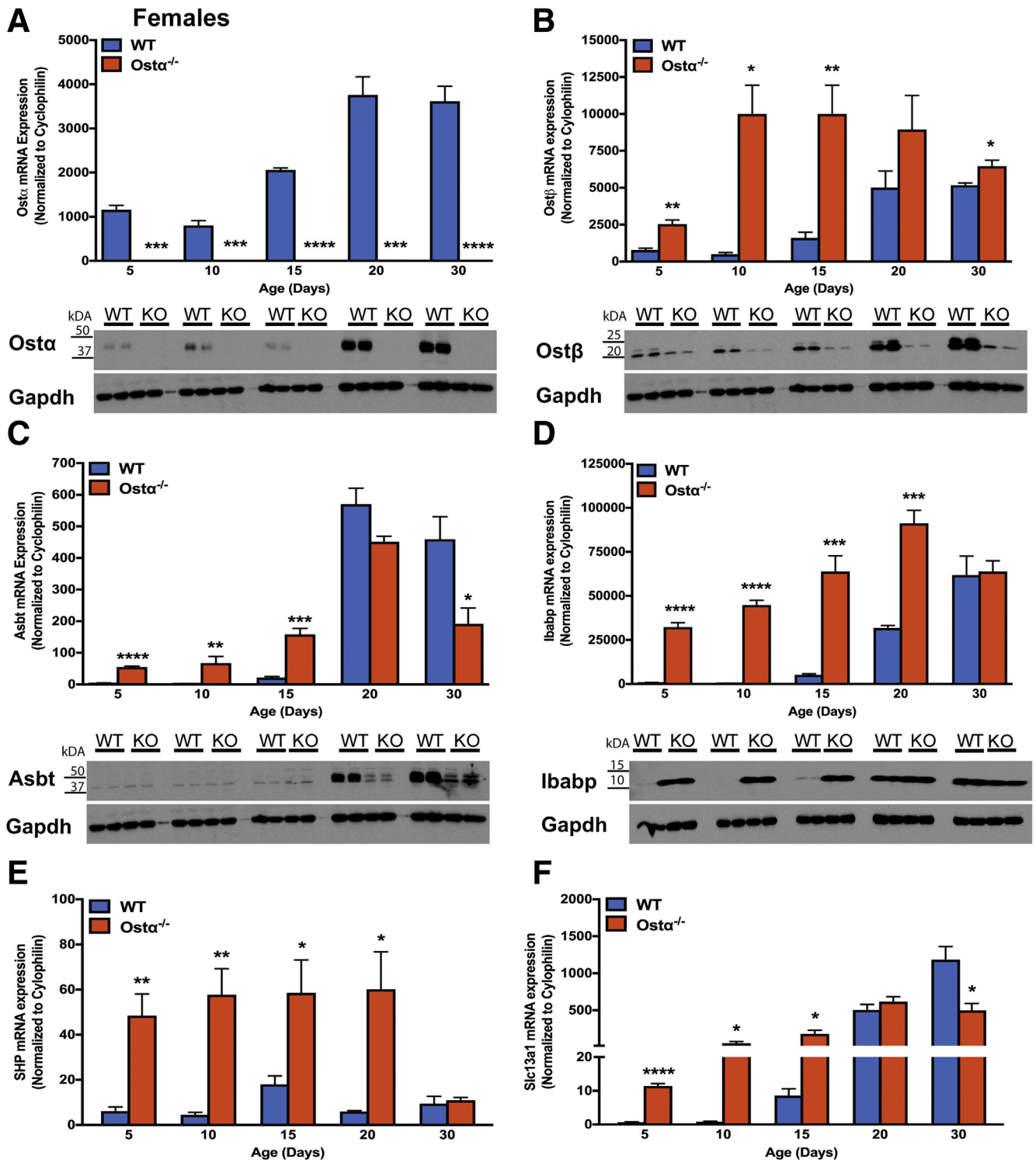


Figure 7. Ontogeny of distal intestinal expression of bile acid transporters and FXR target genes in female WT and Ost $\alpha^{-/-}$ mice. Expression of mRNA and protein for bile acid transport-related genes: (A) *Ost α* , (B) *Ost β* , (C) *Asbt*, and (D) *Ibabp*. Expression of mRNA for FXR target genes: (E) *Shp* and (F) *Slc13a1*. RNA was isolated from the distal small intestine of individual female mice (n = 4–5 per group) and used for real-time PCR analysis. The mRNA expression was normalized using cyclophilin. Mean values \pm SEM are shown. Significant differences between genotypes for that age were as follows: * $P < .05$, ** $P < .01$, *** $P < .001$, and **** $P < .0001$. For protein expression, extracts were prepared from distal intestine from individual mice. Equal amounts of protein from 3 to 5 mice per group were pooled and duplicate samples were subjected to immunoblotting analysis. Blots were re-probed using antibodies to GAPDH as a load control.

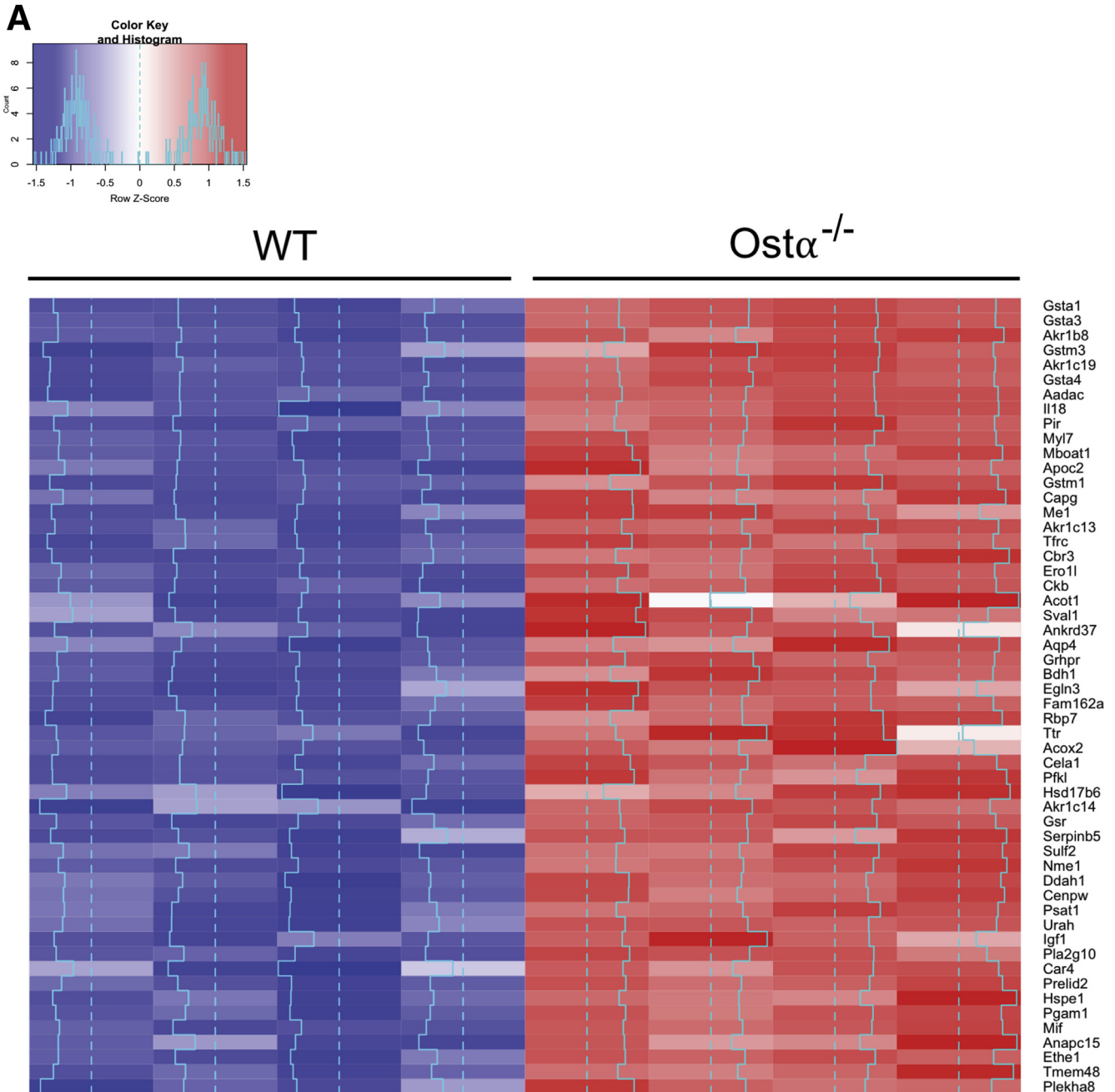


Figure 8. Ileal expression of Nrf2 ARE target genes. (A) Microarray analysis of ileum in adult male WT and $Osta^{-/-}$ mice. Differentially expressed genes whose expression was induced (2-fold change; $P < .05$; $n = 4$) in $Osta^{-/-}$ vs WT mice are shown as a heat map. The blue line indicates the Z score for each gene. (B) Expression of mRNA for Nrf2 target genes in male and female WT and $Osta^{-/-}$ mice. (C) Expression of *Nox1* mRNA in ileum of male and female WT and $Osta^{-/-}$ mice. RNA was isolated from the distal small intestine of individual mice at the indicated ages ($n = 4$ –5 per group) and used for real-time PCR analysis. The mRNA expression was normalized using cyclophilin. Mean values \pm SEM are shown. Significant differences between genotypes for that age and sex were as follows: * $P < .05$, ** $P < .01$, *** $P < .001$, and **** $P < .0001$.

where Nrf2 functions in oxidative stress tolerance,⁵⁰ and in ROS-induced cytoprotective mechanisms in the gut.³⁶ Although invertebrates lack bile acids,⁵¹ we reasoned that the ability of the Nrf2 pathway to respond to bile acids as an environmental insult may be evolutionarily conserved in *Drosophila*. We first examined the sensitivity of adult *Drosophila* to bile acid feeding. The concentration of bile acids

selected for these studies were based on levels measured in the intestinal lumen of human beings and experimental animal models, which are in the millimolar range.^{52–54} However, because the intestine in *Drosophila* is covered by a protective membrane (the peritrophic matrix) and likely lacks transporters for membrane-impermeable conjugated bile acids, the flies were fed unconjugated hydrophobic bile acids, which

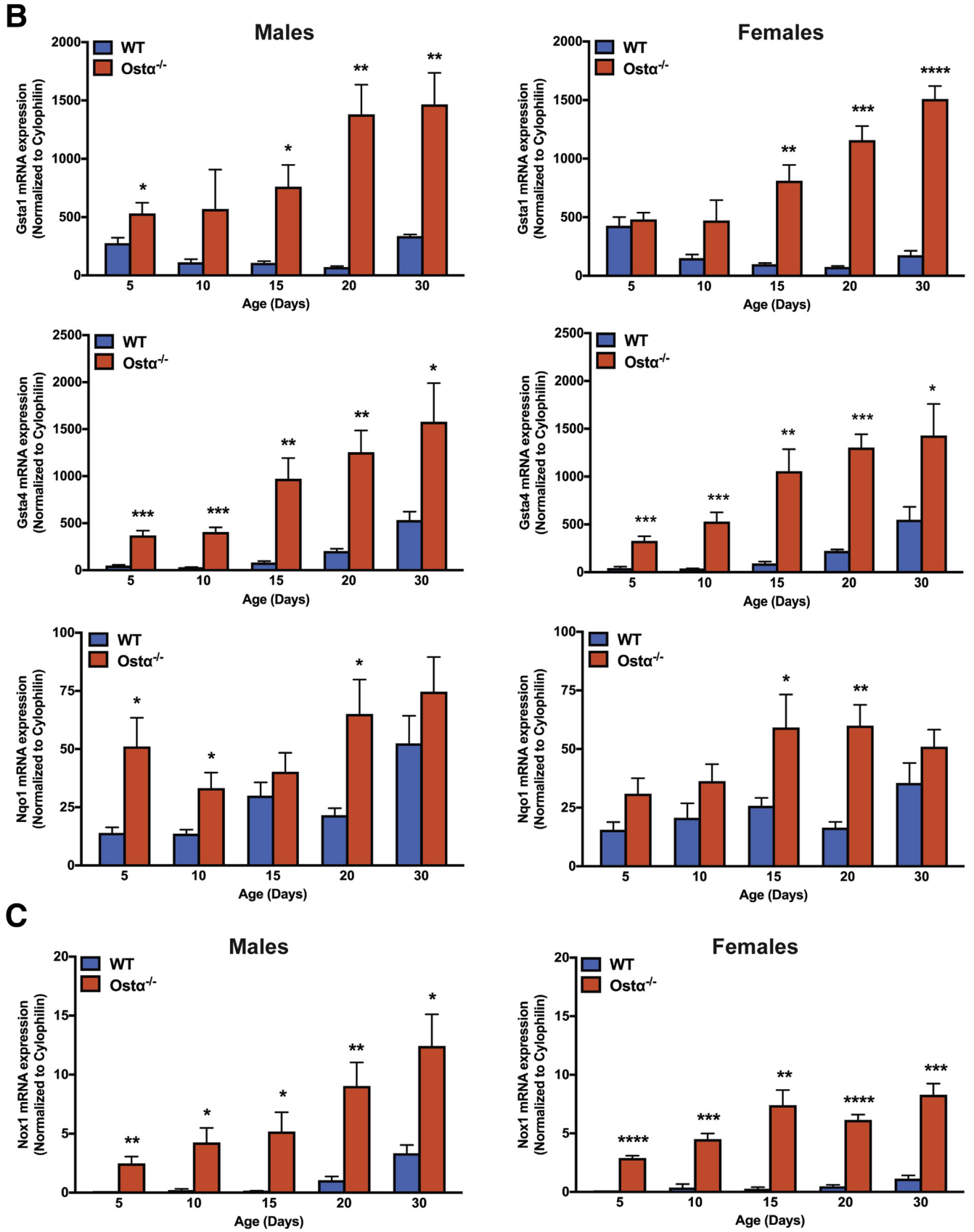


Figure 8. (continued)

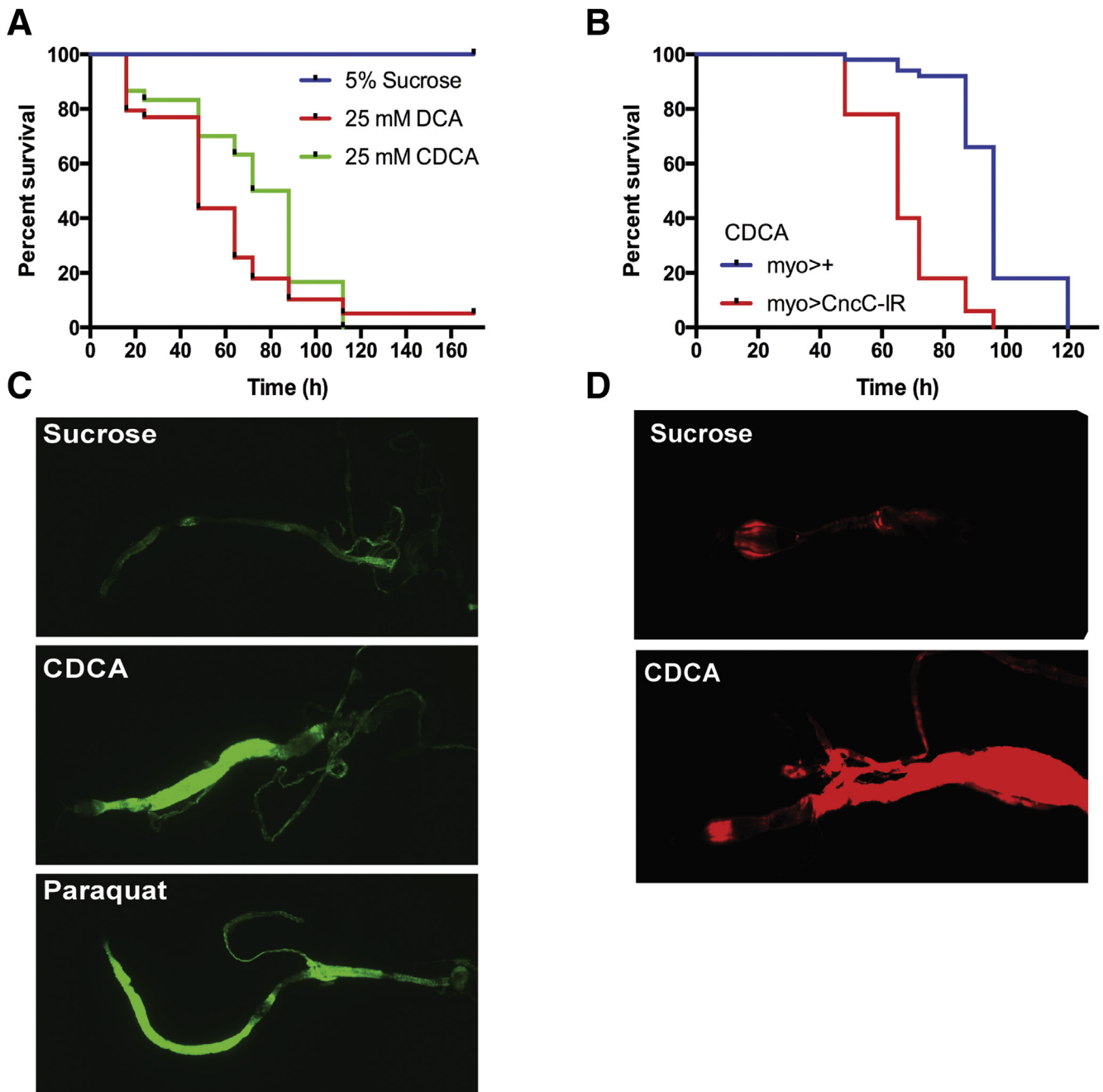


Figure 9. Bile acid cytotoxicity and protective role of intestinal Nrf2 (Cap 'n' collar isoform-c [*cncC*]) in *Drosophila*. (A) Relative survival of 5-day-old adult *Drosophila* in response to feeding CDCA or deoxycholic acid (DCA). Log-rank test for CDCA or DCA vs sucrose, $P < .001$, $n = 30$ – 44 per group. (B) Relative survival of 5-day-old adult *Drosophila* in which the levels of *cncC* (*UAS-CncC^{IR}*) are diminished; log-rank test for *myoA-GAL4* vs *myoA-GAL4*, *UAS-cncC^{IR}*, $P < .0001$, $n = 50$ per group. (C) Detection of ARE-dependent GFP expression in the midgut of *gstD-gfp* adult *Drosophila* fed sucrose, sucrose plus chenodeoxycholic acid, or sucrose plus paraquat. (D) ROS generation in midgut after ingestion of sucrose or sucrose plus 25 mmol/L CDCA. ROS were detected by oxidation of the hydrocyanine ROS-sensitive dye, Hydro-Cy3. Images within a panel were taken at the same confocal settings: original magnification, $20\times$.

would not require a specific transporter for enterocyte uptake. Despite the presence of the peritrophic membrane, we observe reduced survival of adult WT *Drosophila*-fed CDCA at concentrations as low as 6.25 mmol/L, and almost 100% lethality within 100 hours at 25 mmol/L (data not shown). As shown in Figure 9A, feeding the bile acids CDCA or

deoxycholic acid to the flies induced death within 4 days. To examine the potential cytoprotective role of intestinal Nrf2 (known as Cap 'n' collar isoform-c in *Drosophila*), the effect of bile acid feeding on survival of midgut enterocyte-specific Cap 'n' collar isoform-c-deficient *Drosophila* was determined. Reduction of enterocyte Nrf2 expression significantly

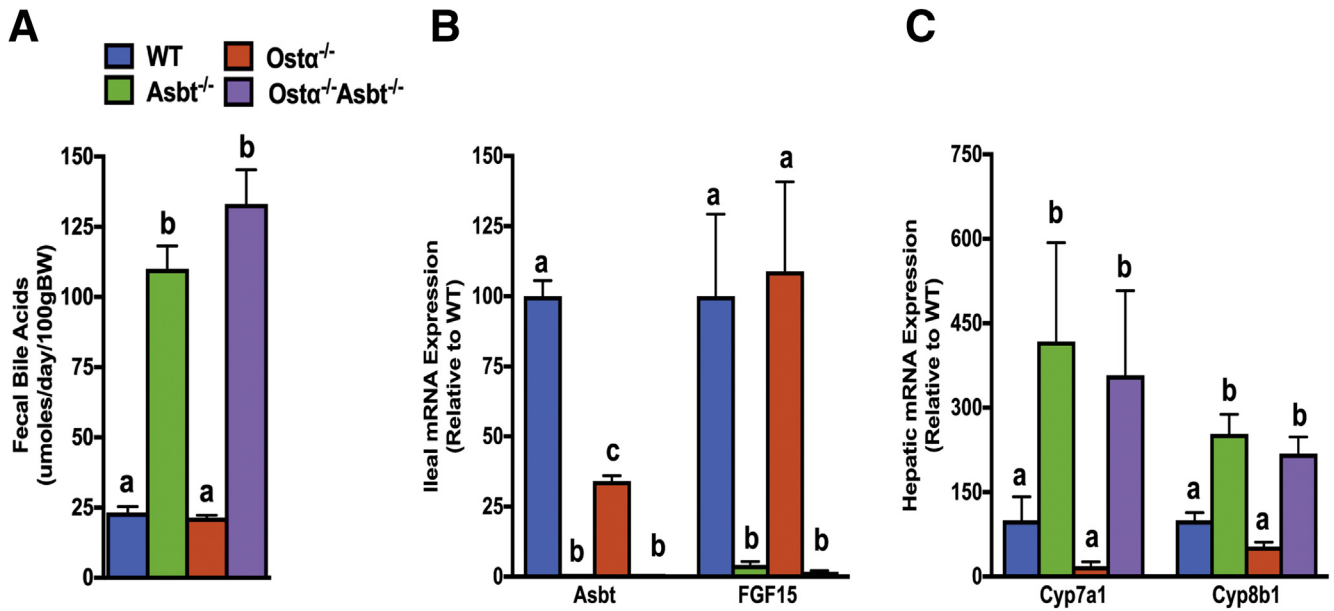


Figure 10. Bile acid metabolism and small intestinal morphologic changes in adult male WT, *Asbt*^{-/-}, *Ost α* ^{-/-}, and *Asbt*^{-/-}*Ost α* ^{-/-} mice. (A) Fecal bile acid excretion. (B) Ileal expression of *Asbt* and *FGF15* mRNA. (C) Hepatic expression of *Cyp7a1* and *Cyp8b1* in adult male mice for the indicated genotypes. The mRNA expression ($n = 5$) was determined by real-time PCR analysis (in triplicate) and normalized using cyclophilin. The mRNA expression is expressed relative to WT (set at 100%). Male mice (age, 8 wk) were included in the analysis ($n = 5$ per genotype). Mean values \pm SEM are shown. Different lowercase letters indicate significant differences ($P < .05$) between genotypes. BW, body weight.

decreased survival further in response to CDCA feeding (Figure 9B). A GFP reporter fly bearing an anti-oxidant response element-dependent promoter (*gstD1-gfp*) that responds to Nrf2 activation then was used to directly determine if bile acid feeding activates the Nrf2-ARE pathway in gut. In that reporter fly model,⁵⁰ feeding CDCA to adult flies induced GFP expression in posterior midgut and hindgut to levels observed for Paraquat, a known inducer of oxidative stress and the Nrf2 pathway (Figure 9C). Because Nrf2 activity can be induced by mechanisms in addition to ROS,⁵⁵ we also examined local generation of ROS in response to bile acid feeding using a redox-sensitive hydrocyanine dye.^{38,56} Fluorescent imaging showed that ingestion of CDCA induced the generation of ROS in midgut (Figure 9D), providing further in vivo evidence that CDCA is a potent activator of the cytoprotective Nrf2 pathway in enterocytes.

Inactivation of the *Asbt* Prevents Ileal Injury in *Ost α* ^{-/-} Mice

The findings suggest that continued *Asbt* activity in the absence of the basolateral bile acid transporter *Ost α -Ost β* leads to ileal accumulation of cytotoxic levels of bile acids early in life, which induces an oxidative stress-related injury and restitution response. To directly test this hypothesis, the *Asbt* null allele was crossed into *Ost α* ^{-/-} mice. In mice, the *Asbt* accounts for the vast majority of bile acid absorption from the gut lumen, with negligible contributions by other mechanisms.⁷ As such, if enterocyte bile acid uptake is required for the intestinal injury/restitution phenotype, inactivation of the *Asbt* should be protective.

The *Ost α* ^{-/-}*Asbt*^{-/-} mice are viable and fertile; crosses between heterozygous mice produced the predicted Mendelian distribution of WT and mutant genotypes. The adult *Ost α* ^{-/-}, *Asbt*^{-/-}, and *Ost α* ^{-/-}*Asbt*^{-/-} mice were indistinguishable from WT mice in terms of survival and gross appearance. To confirm that inactivation of the *Asbt* was sufficient to block intestinal bile acid uptake, fecal bile acid excretion and expression of hepatic and intestinal genes involved in bile acid metabolism were measured. As shown in Figure 10A, fecal bile acid excretion was similar in WT and *Ost α* ^{-/-} mice, and inactivation of the *Asbt* in *Ost α* ^{-/-} mice increased fecal bile acid excretion almost 6-fold to levels observed in *Asbt*^{-/-} mice. In ileum, expression of the *Asbt* was reduced in *Ost α* ^{-/-} mice and undetectable in *Asbt*^{-/-} and *Asbt*^{-/-}*Ost α* ^{-/-} mice. In agreement with the reduced bile acid uptake in the absence of the *Asbt*, expression of ileal *FGF15* mRNA was reduced dramatically in *Ost α* ^{-/-}*Asbt*^{-/-} and *Asbt*^{-/-} mice to almost undetectable levels (Figure 10B). The intestinal bile acid malabsorption was associated with significant increases in the mRNA expression for hepatic *Cyp7a1* and *Cyp8b1*, critical enzymes for bile acid synthesis (Figure 10C).

Because *Ost α -Ost β* shows a gradient of expression along the cephalocaudal axis of the small intestine with highest expression levels in ileum, the segmental intestinal mass was examined in adult mice (age, 2 mo) for the different genotypes. For distal ileum (segment 5), the intestinal weight per unit length was increased significantly (approximately 45%) in male *Ost α* ^{-/-} mice (Figure 11A), and restored to near WT levels in *Ost α* ^{-/-}*Asbt*^{-/-} mice. Histologically, the ileum of postnatal day 10 and adult (age, 8 wk) *Ost α* ^{-/-}*Asbt*^{-/-} mice was almost indistinguishable from WT

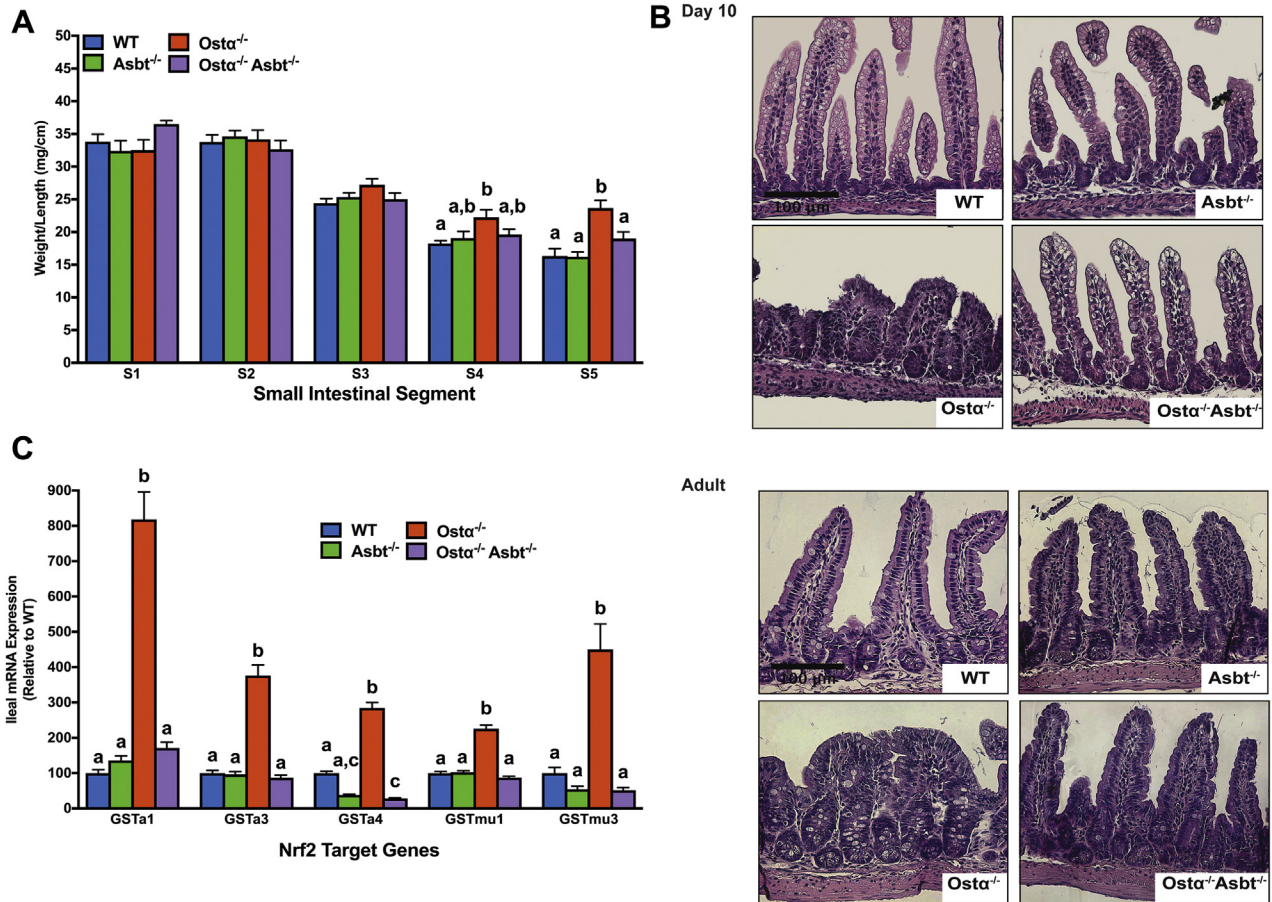


Figure 11. Inactivation of the *Asbt* prevents ileal injury in *Ost $\alpha^{-/-}$* mice. (A) Small intestinal weight per unit length in adult (age, 8 wk) WT, *Asbt $^{-/-}$* , *Ost $\alpha^{-/-}$* , and *Asbt $^{-/-}$ *Ost $\alpha^{-/-}$* male mice. The small intestine was subdivided into 5 equal-length segments and the weight of each is shown as mg/cm length. Mean values \pm SEM ($n = 5$ mice per group) are shown. Distinct lowercase letters indicate significant differences ($P < .05$) between genotypes for that particular intestinal segment. (B) Representative light micrographs of H&E-stained transverse sections of distal small intestine from day 10 and adult (age, 8 wk) WT, *Asbt $^{-/-}$* , *Ost $\alpha^{-/-}$* , and *Asbt $^{-/-}$ *Ost $\alpha^{-/-}$* male mice. Original magnification, 20 \times . Scale bar: 100 μ m. (C) *Gsta1*, *Gsta3*, *Gsta4*, *Gstmu1*, and *Gstmu3* mRNA expression in adult male mice for the indicated genotypes. The mRNA expression ($n = 5$ mice per group) was determined by real-time PCR analysis (in triplicate) and normalized using cyclophilin. The mRNA levels are shown relative to WT (set at 100%). Different lowercase letters indicate significant differences ($P < .05$) between genotypes for that gene.**

mice, showing only mild epithelial reactive changes (Figure 11B). Furthermore, transcript levels of Nrf2 target genes *Gsta1*, *Gsta3*, *Gsta4*, *Gstmu1*, and *Gstmu3* were increased from 3- to 8-fold in adult male *Ost $\alpha^{-/-}$* mice vs WT mice, but reduced to WT levels in the *Ost $\alpha^{-/-}$ *Asbt $^{-/-}$* mice (Figure 11C). Together, these findings provide compelling evidence in support of the hypothesis that continued expression of the *Asbt* in the absence of *Ost α -Ost β* leads to ileal bile acid stasis and injury. In that event, the Nrf2 pathway is one component of the adaptive response that functions to protect the ileal enterocyte from bile acid-induced cytotoxicity.*

Discussion

The major finding of this study was that *Ost α -Ost β* is required to protect the terminal ileum from bile acid-induced injury. We propose that inactivation of *Ost α -Ost β* combined with continued *Asbt* expression results in

bile acid accumulation, injury, and morphologic changes starting in early postnatal development. In a similar fashion, it has been postulated that hepatic *Ost α -Ost β* plays a role in protecting against bile acid accumulation in hepatocytes under cholestatic conditions.^{39,57,58} In *Ost $\alpha^{-/-}$* mice, enterocyte bile acid stasis is associated with significant histologic mucosal alterations, including villous blunting, crypt hyperplasia, increased proliferation, apoptosis, and an increase in the number of mucin-secreting cells at the villous tips. These changes occur in the absence of histologic evidence of necrosis or an active inflammatory response. Despite a mild increase in TNF α mRNA levels early in postnatal development, ileal mRNA levels of TNF α and interleukin 1 β are lower than WT mice by day 30, in agreement with our previous studies of adult *Ost $\alpha^{-/-}$* mice.¹⁰ The mechanisms responsible for the lower ileal cytokine mRNA levels in the postweaning *Ost $\alpha^{-/-}$* mice are unclear, but may be related to persistent increases in Nrf2 and antioxidant activity. For example, previous studies have

shown that administration of L-cysteine can increase intestinal Nrf2 activity, reduce intestinal cytokine levels, and suppress lipopolysaccharide-induced intestinal inflammation in a piglet model.⁵⁹ In addition, intestinal levels of proinflammatory cytokines were found to be higher in Nrf2^{-/-} vs WT mice after traumatic brain injury.⁶⁰

In WT mice or rats, ileal Asbt expression and active bile acid uptake remains low in early postnatal development, increasing after day 15.²⁶⁻²⁸ In contrast, there is an early induction of Asbt expression in Ost α ^{-/-} mice, correlating with increased expression of bile acid-activated FXR target genes, including *Shp* and *Ibabp*. Although premature ileal Asbt expression had been noted previously in mice and rats under pathophysiological conditions such as experimental induction of necrotizing enterocolitis (NEC)^{23,61} or formula feeding,⁶² the underlying cause was not identified. Our attempts to interrogate the pathways/factors known to regulate the Asbt failed to identify a mechanism for the altered ileal Asbt temporal pattern in Ost α ^{-/-} mice. Among those factors that regulate Asbt expression are FXR,^{63,64} GATA4,^{31,65} transthyretin (TTR)/Human antigen R (HuR),^{66,67} and caudal (CDx) transcription factors 1 and 2.⁶⁸ FXR is activated early in postnatal development in Ost α ^{-/-} mice, but is unlikely to be involved because the ileal morphologic changes still are present in Ost α ^{-/-}Fxr^{-/-} mice.¹⁰ GATA4 and TTP/HuR are important regulators of ASBT gene transcription and RNA stability, respectively, in small intestine, and CDX1/2 are important transcriptional regulators of many intestinal genes.⁶⁹ However, the ileal mRNA expression of these factors was similar in male and female WT and Ost α ^{-/-} mice at the early postnatal ages examined (data not shown), arguing against a direct role. Nrf2 has not been reported to directly regulate the Asbt, but Nrf2^{-/-} mice have reduced levels of ileal Asbt expression and bile acid absorption.⁷⁰ That observation raises the possibility that Nrf2 may contribute to the early postnatal increase in Asbt expression in Ost α ^{-/-} mice. However, it also should be noted that the relative increase in Asbt expression is transient and ileal Asbt mRNA and protein expression is reduced in postweaning adult Ost α ^{-/-} mice compared with age-matched WT male or female mice.¹⁰ Finally, these studies have equated ASBT expression with bile acid uptake because the ASBT appears to have a relatively narrow specificity and no endogenous substrates other than bile acids have yet been identified.^{71,72} Although the protection against ileal injury observed in Asbt^{-/-}Ost α ^{-/-} mice supports the hypothesis that the phenotype is secondary to bile acid trapping, it is possible that ASBT transports another solute besides bile acids or its activity is coupled to another cellular pathway, which is responsible for the phenotype.

The cellular and molecular mechanisms of hepatocyte injury caused by retention of hydrophobic bile acids in cholestatic disease have been the subject of intensive study.^{14,15,22} In contrast, less is known regarding the mechanisms and signaling pathways underlying the cytotoxic effects of bile acids in other cell types and in extrahepatic tissues.^{24,73} This is particularly true for ileal enterocytes, which by virtue of their role in the enterohepatic circulation are exposed to a high daily flux of bile acids.⁷⁴ In the 10-day-old Ost α ^{-/-} mice, ileal tissue bile acid levels were increased vs WT mice, and ranged

from approximately 1.5 to 3 μ mol/g of tissue. A limitation of these measurements of tissue-associated bile acids (which are primarily in the mucosa vs muscularis layers) is that it does not distinguish between the extracellular and intracellular compartments or directly measure the bile acid concentrations within the enterocytes. However, the ileal tissue bile acid levels in the 10-day-old Ost α ^{-/-} mice are appreciable and in the range of that observed in liver of bile duct-ligated mice.⁷⁵ In the gut, bile acids such as deoxycholate have been shown to induce apoptosis in colonocytes through mechanisms involving protein kinase C delta⁷⁶ and phospholipase A2,⁷⁷ possibly by altering plasma membrane organization.⁷⁸ Indeed, a myriad of pathways have been implicated in bile acid-induced cytotoxicity, including altering mitochondrial outer membrane structure,⁷⁹ inducing mitochondrial membrane permeability transition,^{43,77,80} activating Nox,^{77,81,82} and signaling via epidermal growth factor receptor and CD95/Fas.^{22,24,83} One of the most important and relevant pathways for this study is bile acid-induced generation of ROS and oxidative stress, secondary to bile acid interaction with plasma membrane enzymes such as Nox and interaction with the mitochondria.⁸⁴⁻⁸⁶ Low to moderate levels of ROS maintain tissue homeostasis and promote cell proliferation and survival,⁸⁷ but higher ROS levels can induce cell damage and death.^{77,81,82,87} In response, cells engage an evolutionarily conserved system, the Nrf2 pathway, to induce expression of a regulon of genes involved in xenobiotic and ROS detoxification, including those involved in glutathione synthesis and utilization, thioredoxin production and utilization, and quinone detoxification.⁸⁷ In vitro studies of cells, including intestine-derived Caco-2 cells, have shown that bile acids can induce ROS⁸⁸ and increase expression of Nrf2-activated genes.⁴⁹ However, activation of Nrf2 by bile acids in enterocytes has not been shown in vivo. In this study, we show that blocking ileal enterocyte bile acid export in Ost α ^{-/-} mice leads to significant induction of Nrf2/ARE cytoprotective gene expression that correlates with the ileal morphologic changes. Tissue ROS levels were not directly measured in this study, but ileal levels of reduced glutathione were found to be decreased in Ost α ^{-/-} mice. In conjunction with the changes in gene expression, these findings suggest that induction of the glutamate-cysteine ligase/glutathione synthetase/GSH axis and expression of glutathione reductase, glutathione peroxidase 2, and glutathione-S-transferase may be quenching ROS or otherwise neutralizing free radicals to protect the epithelium and promote restitution. Exploration of this mechanism in intestine of the reductionist *Drosophila* model directly showed increased generation of ROS, activation of Nrf2-ARE signaling, and reduced survival of midgut enterocyte-specific Nrf2-deficient flies in response to CDCA feeding, supporting the concept of enterocyte bile acid-induced oxidative stress and injury. However, in addition to a pathophysiological role in promoting cell damage, ROS also has a physiologic role in stimulating cell proliferation and tissue restitution.⁸⁹ In particular, there is compelling evidence that ROS generation by Nox1 in the gut epithelium stimulates enterocyte or colonocyte proliferation and is required for restitution and wound repair after mechanical injury or chemical-induced colitis.^{38,47,90-92} In that regard, the significant early induction of Nox1 expression may have a role in promoting ileal mucosal repair in

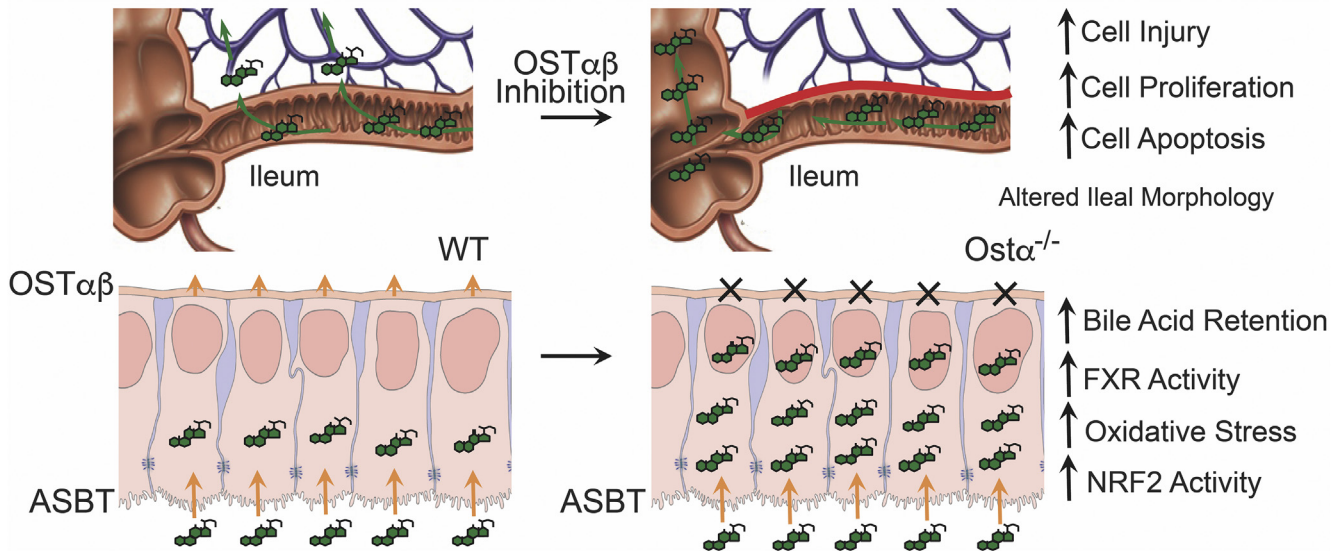


Figure 12. *Ost* α -*Ost* β protects the ileum against bile acid accumulation and bile acid-induced injury. The schematic summarizes our findings. *OST* α -*OST* β functions along with the ASBT to reabsorb bile acids from the ileal lumen and to maintain their enterohepatic circulation. *Ost* α deficiency leads to ileal morphologic changes associated with increased enterocyte proliferation and apoptosis. In the ileal epithelium, loss of *Ost* α leads to increased bile acid retention and increased FXR target gene expression early in postnatal development. This is associated with increased oxidative stress, increased expression of Nrf2/anti-oxidant and cytoprotective genes, and restitution of the epithelium.

Ost α ^{-/-} mice. Although the adaptive mechanisms are not sufficient to restore the ileal morphology back to that of the WT mice, it should be noted that the *Ost* α ^{-/-} mice survive and continue to thrive. The persistence of the ileal morphologic changes may be because the hypothesized offending agent, bile acids, continuously are synthesized and secreted into the small intestine over the life of the mouse. As a result, an unremitting but controlled cycle of epithelial injury and restitution ensues. A schematic summarizing the findings and proposed mechanisms underlying the intestinal changes associated with loss of *Ost* α is shown in Figure 12.

In theory, enterocyte injury secondary to imbalanced expression of the ASBT and *OST* α -*OST* β may be involved in human disease. For example, this mechanism may contribute to the pathogenesis of NEC because ASBT expression has been reported to be higher in premature infants diagnosed with NEC vs premature infants with non-NEC diagnoses.⁶¹ Furthermore, in rat and mouse models of NEC, ileal damage correlated with increased *Asbt* expression and intracellular bile acid accumulation, and administration of an ASBT inhibitor or inactivation of the *Asbt* gene was protective.^{23,61} By comparison with the NEC models, the intestinal phenotype is relatively mild in *Ost* α ^{-/-} mice, although the pups are born full-term and dam-fed, raising the possibility that the neonatal *Ost* α ^{-/-} mice may be particularly susceptible to additional stressors such as hypoxia or formula feeding. Outside of inflammatory bowel disease, ileal atrophy is not often seen without accompanying duodenojejunal changes,⁹³ but cases of apparent primary ileal villous atrophy and bile acid malabsorption of unknown etiology have been reported.⁹⁴⁻⁹⁶ Although the relationship of these disorders and the intestinal bile acid transporters remains to be determined, it should be noted that an inherited *OST* β (*SLC51B*) deficiency recently

was identified in a family with 2 affected brothers. These pediatric patients presented with congenital diarrhea, fat-soluble vitamin deficiency, and increased liver serum chemistries.⁹⁷ Although a cursory endoscopic examination showed no obvious ileal abnormalities in the older affected sibling, additional studies will be required to determine the mechanisms underlying the patients' diarrhea and apparent steatorrhea. Their clinical presentation may be owing solely to bile acid malabsorption and reduced luminal bile acid concentrations, similar to patients with ASBT mutations.^{5,6} Alternatively, changes in the ultrastructure of the ileal mucosa secondary to imbalanced ASBT and *OST* α -*OST* β expression also may contribute to the phenotype.

In conclusion, we have provided data indicating that in addition to its role in maintaining the enterohepatic circulation of bile acids, *Ost* α -*Ost* β appears to play a major role in protecting the ileal epithelium against bile acid accumulation and injury. Inactivation of *Ost* α resulted in increased expression of FXR target genes as well as villous blunting, cell apoptosis, and oxidative stress in early postnatal development. There is also an early robust induction of Nrf2 anti-oxidant and cytoprotective target genes, which may be involved in the subsequent healing and restitution response.

References

- Boyer JL. Bile formation and secretion. *Compr Physiol* 2013;3:1035-1078.
- Dawson PA, Karpen SJ. Intestinal transport and metabolism of bile acids. *J Lipid Res* 2015;56:1085-1099.
- Dawson PA, Hubbert M, Haywood J, Craddock AL, Zerangue N, Christian WV, Ballatori N. The heteromeric organic solute transporter alpha-beta, *Ost* α -*Ost* β ,

- is an ileal basolateral bile acid transporter. *J Biol Chem* 2005;280:6960–6968.
4. Ballatori N, Christian WV, Lee JY, Dawson PA, Soroka CJ, Boyer JL, Madejczyk MS, Li N. OSTalpha-OSTbeta: a major basolateral bile acid and steroid transporter in human intestinal, renal, and biliary epithelia. *Hepatology* 2005;42:1270–1279.
 5. Heubi JE, Balistreri WF, Fondacaro JD, Partin JC, Schubert WK. Primary bile acid malabsorption: defective in vitro ileal active bile acid transport. *Gastroenterology* 1982;83:804–811.
 6. Oelkers P, Kirby LC, Heubi JE, Dawson PA. Primary bile acid malabsorption caused by mutations in the ileal sodium-dependent bile acid transporter gene (SLC10A2). *J Clin Invest* 1997;99:1880–1887.
 7. Dawson PA, Haywood J, Craddock AL, Wilson M, Tietjen M, Kluckman K, Maeda N, Parks JS. Targeted deletion of the ileal bile acid transporter eliminates enterohepatic cycling of bile acids in mice. *J Biol Chem* 2003;278:33920–33927.
 8. Rao A, Haywood J, Craddock AL, Belinsky MG, Kruh GD, Dawson PA. The organic solute transporter alpha-beta, Ostalpha-Ostbeta, is essential for intestinal bile acid transport and homeostasis. *Proc Natl Acad Sci U S A* 2008;105:3891–3896.
 9. Ballatori N, Fang F, Christian WV, Li N, Hammond CL. Ostalpha-Ostbeta is required for bile acid and conjugated steroid disposition in the intestine, kidney, and liver. *Am J Physiol Gastrointest Liver Physiol* 2008;295:G179–G186.
 10. Lan T, Rao A, Haywood J, Kock ND, Dawson PA. Mouse organic solute transporter alpha deficiency alters FGF15 expression and bile acid metabolism. *J Hepatol* 2012;57:359–365.
 11. Lan T, Haywood J, Rao A, Dawson PA. Molecular mechanisms of altered bile acid homeostasis in organic solute transporter-alpha knockout mice. *Dig Dis* 2011;29:18–22.
 12. Koch S, Nusrat A. The life and death of epithelia during inflammation: lessons learned from the gut. *Annu Rev Pathol* 2012;7:35–60.
 13. Hofmann AF. The continuing importance of bile acids in liver and intestinal disease. *Arch Intern Med* 1999;159:2647–2658.
 14. Malhi H, Guicciardi ME, Gores GJ. Hepatocyte death: a clear and present danger. *Physiol Rev* 2010;90:1165–1194.
 15. Cai SY, Ouyang X, Chen Y, Soroka CJ, Wang J, Mennone A, Wang Y, Mehal WZ, Jain D, Boyer JL. Bile acids initiate cholestatic liver injury by triggering a hepatocyte-specific inflammatory response. *JCI Insight* 2017;2:e90780.
 16. Pawlikowska L, Strautnieks S, Jankowska I, Czubkowski P, Emerick K, Antoniou A, Wanty C, Fischler B, Jacquemin E, Wali S, Blanchard S, Nielsen IM, Bourke B, McQuaid S, Lacaille F, Byrne JA, van Eerde AM, Kolho KL, Klomp L, Houwen R, Bacchetti P, Lobritto S, Hupertz V, McClean P, Mieli-Vergani G, Shneider B, Nemeth A, Sokal E, Freimer NB, Knisely AS, Rosenthal P, Whittington PF, Pawlowska J, Thompson RJ, Bull LN. Differences in presentation and progression between severe FIC1 and BSEP deficiencies. *J Hepatol* 2010;53:170–178.
 17. Bochkis IM, Rubins NE, White P, Furth EE, Friedman JR, Kaestner KH. Hepatocyte-specific ablation of Foxa2 alters bile acid homeostasis and results in endoplasmic reticulum stress. *Nat Med* 2008;14:828–836.
 18. Tamaki N, Hatano E, Taura K, Tada M, Kodama Y, Nitta T, Iwaisako K, Seo S, Nakajima A, Ikai I, Uemoto S. CHOP deficiency attenuates cholestasis-induced liver fibrosis by reduction of hepatocyte injury. *Am J Physiol Gastrointest Liver Physiol* 2008;294:G498–G505.
 19. Henkel AS, LeCuyer B, Olivares S, Green RM. Endoplasmic reticulum stress regulates hepatic bile acid metabolism in mice. *Cell Mol Gastroenterol Hepatol* 2017;3:261–271.
 20. Yerushalmi B, Dahl R, Devereaux MW, Gumprich E, Sokol RJ. Bile acid-induced rat hepatocyte apoptosis is inhibited by antioxidants and blockers of the mitochondrial permeability transition. *Hepatology* 2001;33:616–626.
 21. Li M, Cai SY, Boyer JL. Mechanisms of bile acid mediated inflammation in the liver. *Mol Aspects Med* 2017;56:45–53.
 22. Perez MJ, Briz O. Bile-acid-induced cell injury and protection. *World J Gastroenterol* 2009;15:1677–1689.
 23. Halpern MD, Holubec H, Saunders TA, Dvorak K, Clark JA, Doelle SM, Ballatori N, Dvorak B. Bile acids induce ileal damage during experimental necrotizing enterocolitis. *Gastroenterology* 2006;130:359–372.
 24. Barrasa JI, Olmo N, Lizarbe MA, Turnay J. Bile acids in the colon, from healthy to cytotoxic molecules. *Toxicol In Vitro* 2013;27:964–977.
 25. Shneider BL, Dawson PA, Christie DM, Hardikar W, Wong MH, Suchy FJ. Cloning and molecular characterization of the ontogeny of a rat ileal sodium-dependent bile acid transporter. *J Clin Invest* 1995;95:745–754.
 26. Cui JY, Aleksunes LM, Tanaka Y, Fu ZD, Guo Y, Guo GL, Lu H, Zhong XB, Klaassen CD. Bile acids via FXR initiate the expression of major transporters involved in the enterohepatic circulation of bile acids in newborn mice. *Am J Physiol Gastrointest Liver Physiol* 2012;302:G979–G996.
 27. Shneider BL, Setchell KD, Crossman MW. Fetal and neonatal expression of the apical sodium-dependent bile acid transporter in the rat ileum and kidney. *Pediatr Res* 1997;42:189–194.
 28. Christie DM, Dawson PA, Thevananther S, Shneider BL. Comparative analysis of the ontogeny of a sodium-dependent bile acid transporter in rat kidney and ileum. *Am J Physiol* 1996;271:G377–G385.
 29. McFarlane L, Truong V, Palmer JS, Wilhelm D. Novel PCR assay for determining the genetic sex of mice. *Sex Dev* 2013;7:207–211.
 30. Schindelin J, Arganda-Carreras I, Frise E, Kaynig V, Longair M, Pietzsch T, Preibisch S, Rueden C, Saalfeld S, Schmid B, Tinevez JY, White DJ, Hartenstein V, Eliceiri K, Tomancak P, Cardona A. Fiji: an open-source platform for biological-image analysis. *Nat Methods* 2012;9:676–682.

31. Beuling E, Kerkhof IM, Nicksa GA, Giuffrida MJ, Haywood J, aan de Kerk DJ, Piaseckyj CM, Pu WT, Buchmiller TL, Dawson PA, Krasinski SD. Conditional Gata4 deletion in mice induces bile acid absorption in the proximal small intestine. *Gut* 2010;59:888–895.
32. Jones DP, Mody VC Jr, Carlson JL, Lynn MJ, Sternberg P Jr. Redox analysis of human plasma allows separation of pro-oxidant events of aging from decline in antioxidant defenses. *Free Radic Biol Med* 2002;33:1290–1300.
33. Tian J, Brown LA, Jones DP, Levin MS, Wang L, Rubin DC, Ziegler TR. Intestinal redox status of major intracellular thiols in a rat model of chronic alcohol consumption. *JPEN J Parenter Enteral Nutr* 2009;33:662–668.
34. Irizarry RA, Hobbs B, Collin F, Beazer-Barclay YD, Antonellis KJ, Scherf U, Speed TP. Exploration, normalization, and summaries of high density oligonucleotide array probe level data. *Biostatistics* 2003;4:249–264.
35. Huang da W, Sherman BT, Lempicki RA. Systematic and integrative analysis of large gene lists using DAVID bioinformatics resources. *Nat Protoc* 2009;4:44–57.
36. Jones RM, Desai C, Darby TM, Luo L, Wolfarth AA, Scharer CD, Ardita CS, Reedy AR, Keebaugh ES, Neish AS. Lactobacilli modulate epithelial cytoprotection through the Nrf2 pathway. *Cell Rep* 2015;12:1217–1225.
37. Luo L, Reedy AR, Jones RM. Detecting reactive oxygen species generation and stem cell proliferation in the *Drosophila* Intestine. *Methods Mol Biol* 2016;1422:103–113.
38. Jones RM, Luo L, Ardita CS, Richardson AN, Kwon YM, Mercante JW, Alam A, Gates CL, Wu H, Swanson PA, Lambeth JD, Denning PW, Neish AS. Symbiotic lactobacilli stimulate gut epithelial proliferation via Nox-mediated generation of reactive oxygen species. *EMBO J* 2013;32:3017–3028.
39. Soroka CJ, Mennone A, Hagey LR, Ballatori N, Boyer JL. Mouse organic solute transporter alpha deficiency enhances renal excretion of bile acids and attenuates cholestasis. *Hepatology* 2010;51:181–190.
40. Soroka CJ, Velazquez H, Mennone A, Ballatori N, Boyer JL. Ostalpha depletion protects liver from oral bile acid load. *Am J Physiol Gastrointest Liver Physiol* 2011;301:G574–G579.
41. Jenkins SL, Wang J, Vazir M, Vela J, Sahagun O, Gabbay P, Hoang L, Diaz RL, Aranda R, Martin MG. Role of passive and adaptive immunity in influencing enterocyte-specific gene expression. *Am J Physiol Gastrointest Liver Physiol* 2003;285:G714–G725.
42. Li N, Cui Z, Fang F, Lee JY, Ballatori N. Heterodimerization, trafficking and membrane topology of the two proteins, Ost alpha and Ost beta, that constitute the organic solute and steroid transporter. *Biochem J* 2007;407:363–372.
43. Palmeira CM, Rolo AP. Mitochondrially-mediated toxicity of bile acids. *Toxicology* 2004;203:1–15.
44. Woolbright BL, Jaeschke H. Novel insight into mechanisms of cholestatic liver injury. *World J Gastroenterol* 2012;18:4985–4993.
45. Ma Q. Role of nrf2 in oxidative stress and toxicity. *Annu Rev Pharmacol Toxicol* 2013;53:401–426.
46. Esworthy RS, Kim BW, Chow J, Shen B, Doroshov JH, Chu FF. Nox1 causes ileocolitis in mice deficient in glutathione peroxidase-1 and -2. *Free Radic Biol Med* 2014;68:315–325.
47. Leoni G, Alam A, Neumann PA, Lambeth JD, Cheng G, McCoy J, Hilgarth RS, Kundu K, Murthy N, Kusters D, Reutelingsperger C, Perretti M, Parkos CA, Neish AS, Nusrat A. Annexin A1, formyl peptide receptor, and NOX1 orchestrate epithelial repair. *J Clin Invest* 2013;123:443–454.
48. Lambeth JD, Neish AS. Nox enzymes and new thinking on reactive oxygen: a double-edged sword revisited. *Annu Rev Pathol* 2014;9:119–145.
49. Tan KP, Yang M, Ito S. Activation of nuclear factor (erythroid-2 like) factor 2 by toxic bile acids provokes adaptive defense responses to enhance cell survival at the emergence of oxidative stress. *Mol Pharmacol* 2007;72:1380–1390.
50. Sykiotis GP, Bohmann D. Keap1/Nrf2 signaling regulates oxidative stress tolerance and lifespan in *Drosophila*. *Dev Cell* 2008;14:76–85.
51. Haslewood GA. Bile salt evolution. *J Lipid Res* 1967;8:535–550.
52. Dietschy JM. The role of bile salts in controlling the rate of intestinal cholesterologenesis. *J Clin Invest* 1968;47:286–300.
53. Northfield TC, McColl I. Postprandial concentrations of free and conjugated bile acids down the length of the normal human small intestine. *Gut* 1973;14:513–518.
54. Campbell NB, Ruaux CG, Shifflett DE, Steiner JM, Williams DA, Bliklager AT. Physiological concentrations of bile salts inhibit recovery of ischemic-injured porcine ileum. *Am J Physiol Gastrointest Liver Physiol* 2004;287:G399–G407.
55. Chatterjee N, Tian M, Spirohn K, Boutros M, Bohmann D. Keap1-independent regulation of Nrf2 activity by protein acetylation and a BET bromodomain protein. *PLoS Genet* 2016;12:e1006072.
56. Kundu K, Knight SF, Willett N, Lee S, Taylor WR, Murthy N. Hydrocyanines: a class of fluorescent sensors that can image reactive oxygen species in cell culture, tissue, and in vivo. *Angew Chem Int Ed Engl* 2009;48:299–303.
57. Boyer JL, Trauner M, Mennone A, Soroka CJ, Cai SY, Moustafa T, Zollner G, Lee JY, Ballatori N. Upregulation of a basolateral FXR-dependent bile acid efflux transporter OSTalpha-OSTbeta in cholestasis in humans and rodents. *Am J Physiol Gastrointest Liver Physiol* 2006;290:G1124–G1130.
58. Soroka CJ, Ballatori N, Boyer JL. Organic solute transporter, OSTalpha-OSTbeta: its role in bile acid transport and cholestasis. *Semin Liver Dis* 2010;30:178–185.
59. Song Z, Tong G, Xiao K, Jiao F, Ke Y, Hu C. L-cysteine protects intestinal integrity, attenuates intestinal inflammation and oxidant stress, and modulates NF-kappaB and Nrf2 pathways in weaned piglets after LPS challenge. *Innate Immun* 2016;22:152–161.
60. Jin W, Wang H, Ji Y, Hu Q, Yan W, Chen G, Yin H. Increased intestinal inflammatory response and gut

- barrier dysfunction in Nrf2-deficient mice after traumatic brain injury. *Cytokine* 2008;44:135–140.
61. Halpern MD, Weitkamp JH, Patrick SKM, Dobrenen HJ, Khailova L, Correa H, Dvorak B. Apical sodium-dependent bile acid transporter upregulation is associated with necrotizing enterocolitis. *Am J Physiol Gastrointest Liver Physiol* 2010;299:G623–G631.
 62. Schuck-Phan A, Phan T, Dawson PA, Dial EJ, Bell C, Liu Y, Rhoads JM, Lichtenberger LM. Formula feeding predisposes gut to NSAID-induced small intestinal injury. *Clin Exp Pharmacol* 2016;6:222.
 63. Chen F, Ma L, Ananthanarayanan M, Sinal C, Dawson P, Mangelsdorf D, Gonzalez F, Shneider BL. Negative-feedback regulation of the ileal apical sodium-dependent bile acid transporter (ASBT) is mediated by the farnesoid x-receptor (FXR). *Gastroenterology* 2002;122:A625-A.
 64. Neimark E, Chen F, Li X, Shneider BL. Bile acid-induced negative feedback regulation of the human ileal bile acid transporter. *Hepatology* 2004;40:149–156.
 65. Battle MA, Bondow BJ, Iverson MA, Adams SJ, Jandacek RJ, Tso P, Duncan SA. GATA4 is essential for jejunal function in mice. *Gastroenterology* 2008;135:1676–1686 e1.
 66. Chen F, Shyu AB, Shneider BL. Hu antigen R and tristetraprolin: counter-regulators of rat apical sodium-dependent bile acid transporter by way of effects on messenger RNA stability. *Hepatology* 2011;54:1371–1378.
 67. Soler DM, Ghosh A, Chen F, Shneider BL. A single element in the 3'UTR of the apical sodium-dependent bile acid transporter controls both stabilization and destabilization of mRNA. *Biochem J* 2014;462:547–553.
 68. Ma L, Juttner M, Kullak-Ublick GA, Eloranta JJ. Regulation of the gene encoding the intestinal bile acid transporter ASBT by the caudal-type homeobox proteins CDX1 and CDX2. *Am J Physiol Gastrointest Liver Physiol* 2012;302:G123–G133.
 69. Verzi MP, Shin H, Ho LL, Liu XS, Shivdasani RA. Essential and redundant functions of caudal family proteins in activating adult intestinal genes. *Mol Cell Biol* 2011;31:2026–2039.
 70. Weerachayaphorn J, Mennone A, Soroka CJ, Harry K, Hagey LR, Kensler TW, Boyer JL. Nuclear factor-E2-related factor 2 is a major determinant of bile acid homeostasis in the liver and intestine. *Am J Physiol Gastrointest Liver Physiol* 2012;302:G925–G936.
 71. Kramer W, Stengelin S, Baringhaus KH, Enhsen A, Heuer H, Becker W, Corsiero D, Girbig F, Noll R, Weyland C. Substrate specificity of the ileal and the hepatic Na(+)/bile acid cotransporters of the rabbit. I. Transport studies with membrane vesicles and cell lines expressing the cloned transporters. *J Lipid Res* 1999;40:1604–1617.
 72. Craddock AL, Love MW, Daniel RW, Kirby LC, Walters HC, Wong MH, Dawson PA. Expression and transport properties of the human ileal and renal sodium-dependent bile acid transporter. *Am J Physiol* 1998;274:G157–G169.
 73. Fickert P, Krones E, Pollheimer MJ, Thueringer A, Moustafa T, Silbert D, Halilbasic E, Yang M, Jaeschke H, Stokman G, Wells RG, Eller K, Rosenkranz AR, Eggertsen G, Wagner CA, Langner C, Denk H, Trauner M. Bile acids trigger cholemic nephropathy in common bile-duct-ligated mice. *Hepatology* 2013;58:2056–2069.
 74. Marcus SN, Schteingart CD, Marquez ML, Hofmann AF, Xia Y, Steinbach JH, Ton-Nu HT, Lillienau J, Angellotti MA, Schmassmann A. Active absorption of conjugated bile acids in vivo. Kinetic parameters and molecular specificity of the ileal transport system in the rat. *Gastroenterology* 1991;100:212–221.
 75. Wang L, Hartmann P, Haimerl M, Bathena SP, Sjowall C, Almer S, Alnouti Y, Hofmann AF, Schnabl B. Nod2 deficiency protects mice from cholestatic liver disease by increasing renal excretion of bile acids. *J Hepatol* 2014;60:1259–1267.
 76. Looby E, Long A, Kelleher D, Volkov Y. Bile acid deoxycholate induces differential subcellular localisation of the PKC isoenzymes beta 1, epsilon and delta in colonic epithelial cells in a sodium butyrate insensitive manner. *Int J Cancer* 2005;114:887–895.
 77. Barrasa JI, Olmo N, Perez-Ramos P, Santiago-Gomez A, Lecona E, Turnay J, Lizarbe MA. Deoxycholic and chenodeoxycholic bile acids induce apoptosis via oxidative stress in human colon adenocarcinoma cells. *Apoptosis* 2011;16:1054–1067.
 78. Mello-Vieira J, Sousa T, Coutinho A, Fedorov A, Lucas SD, Moreira R, Castro RE, Rodrigues CM, Prieto M, Fernandes F. Cytotoxic bile acids, but not cytoprotective species, inhibit the ordering effect of cholesterol in model membranes at physiologically active concentrations. *Biochim Biophys Acta* 2013;1828:2152–2163.
 79. Sousa T, Castro RE, Pinto SN, Coutinho A, Lucas SD, Moreira R, Rodrigues CM, Prieto M, Fernandes F. Deoxycholic acid modulates cell death signaling through changes in mitochondrial membrane properties. *J Lipid Res* 2015;56:2158–2171.
 80. Payne CM, Weber C, Crowley-Skillicorn C, Dvorak K, Bernstein H, Bernstein C, Holubec H, Dvorakova B, Garewal H. Deoxycholate induces mitochondrial oxidative stress and activates NF-kappaB through multiple mechanisms in HCT-116 colon epithelial cells. *Carcinogenesis* 2007;28:215–222.
 81. Li D, Cao WB. Bile acid receptor TGR5, NADPH Oxidase NOX5-S and CREB mediate bile acid-induced DNA damage in Barrett's esophageal adenocarcinoma cells. *Sci Rep* 2016;6:31538.
 82. Bernstein H, Holubec H, Bernstein C, Ignatenko NA, Gerner E, Dvorak K, Besselsen D, Blohm-Mangone KA, Padilla-Torres J, Dvorakova B, Garewal H, Payne CM. Deoxycholate-induced colitis is markedly attenuated in Nos2 knockout mice in association with modulation of gene expression profiles. *Dig Dis Sci* 2007;52:628–642.
 83. Dossa AY, Escobar O, Golden J, Frey MR, Ford HR, Gayer CP. Bile acids regulate intestinal cell proliferation by modulating EGFR and FXR signaling. *Am J Physiol Gastrointest Liver Physiol* 2016;310:G81–G92.
 84. Lechner S, Muller-Ladner U, Schlottmann K, Jung B, McClelland M, Ruschoff J, Welsh J, Scholmerich J,

- Kullmann F. Bile acids mimic oxidative stress induced upregulation of thioredoxin reductase in colon cancer cell lines. *Carcinogenesis* 2002;23:1281–1288.
85. Cosentino-Gomes D, Rocco-Machado N, Meyer-Fernandes JR. Cell signaling through protein kinase C oxidation and activation. *Int J Mol Sci* 2012; 13:10697–10721.
 86. Dikalov S. Cross talk between mitochondria and NADPH oxidases. *Free Radic Biol Med* 2011;51:1289–1301.
 87. Gorrini C, Harris IS, Mak TW. Modulation of oxidative stress as an anticancer strategy. *Nat Rev Drug Discov* 2013;12:931–947.
 88. Araki Y, Katoh T, Ogawa A, Bamba S, Andoh A, Koyama S, Fujiyama Y, Bamba T. Bile acid modulates transepithelial permeability via the generation of reactive oxygen species in the Caco-2 cell line. *Free Radic Biol Med* 2005;39:769–780.
 89. Ray PD, Huang BW, Tsuji Y. Reactive oxygen species (ROS) homeostasis and redox regulation in cellular signaling. *Cell Signal* 2012;24:981–990.
 90. Coant N, Ben Mkaddem S, Pedruzzi E, Guichard C, Treton X, Ducroc R, Freund JN, Cazals-Hatem D, Bouhnik Y, Woerther PL, Skurnik D, Grodet A, Fay M, Biard D, Lesuffleur T, Deffert C, Moreau R, Groyer A, Krause KH, Daniel F, Ogier-Denis E. NADPH oxidase 1 modulates WNT and NOTCH1 signaling to control the fate of proliferative progenitor cells in the colon. *Mol Cell Biol* 2010;30:2636–2650.
 91. Kato M, Marumo M, Nakayama J, Matsumoto M, Yabe-Nishimura C, Kamata T. The ROS-generating oxidase Nox1 is required for epithelial restitution following colitis. *Exp Anim* 2016;65:197–205.
 92. Alam A, Leoni G, Wentworth CC, Kwal JM, Wu H, Ardita CS, Swanson PA, Lambeth JD, Jones RM, Nusrat A, Neish AS. Redox signaling regulates commensal-mediated mucosal homeostasis and restitution and requires formyl peptide receptor 1. *Mucosal Immunol* 2014;7:645–655.
 93. Halphen M, Galian A, Certin M, Ink F, Filali A, Rambaud JC. Clinicopathological study of a patient with idiopathic villous atrophy and small vessel alterations of the ileum. *Dig Dis Sci* 1989;34:111–117.
 94. Popovic OS, Kostic KM, Milovic VB, Milutinovic-Djuric S, Miletic VD, Sestic L, Djordjevic M, Bulajic M, Bojic P, Rubinic M, et al. Primary bile acid malabsorption. Histologic and immunologic study in three patients. *Gastroenterology* 1987;92:1851–1858.
 95. Marteau P, Lavergne-Slove A, Lemann M, Bouhnik Y, Bertheau P, Becheur H, Galian A, Rambaud JC. Primary ileal villous atrophy is often associated with microscopic colitis. *Gut* 1997;41:561–564.
 96. Milutinovic-Djuric S, Popovic OS, Milovic V, Necic D, Kostic KM. Postcholecystectomy diarrhea from villous atrophy of the terminal ileum. *J Clin Gastroenterol* 1993; 16:227–230.
 97. Sultan M, Rao A, Elpeleg O, Vaz FM, Abu Libdeh BY, Karpen SJ, Dawson PA. Organic solute transporter-beta (SLC51B) deficiency in two brothers with congenital diarrhea and features of cholestasis. *Hepatology* 2017, Epub ahead of print.

Received June 2, 2017. Accepted January 5, 2018.

Correspondence

Address correspondence to: Paul A. Dawson, PhD, Division of Pediatric Gastroenterology, Hepatology and Nutrition, Emory University School of Medicine, Health Sciences Research Building, 1760 Haygood Drive, Suite E200, Office E206, Atlanta, Georgia 30322. e-mail: paul.dawson@emory.edu; fax: (404) 727-5737.

Acknowledgments

The authors thank Lou Craddock at the Wake Forest School of Medicine Cancer Genomics Shared Resource for expert technical assistance with the microarray studies, and Dr Neil Anthony at the Emory University Integrated Cellular Imaging Core for assistance and helpful discussions.

Current address of C.F.: Department of Pathology and Laboratory Medicine, Yerkes National Primate Research Center, Emory University, Atlanta, Georgia; present address of B.H.H.: Department of Pathology, University of Cincinnati Medical Center, Cincinnati, Ohio.

Author contributions

Courtney Ferrebee, Paul Dawson, Brian Robinson, and Rheinalt Jones were responsible for the study concept and design; Courtney Ferrebee, Jianing Li, Jamie Haywood, Kimberly Pachura, Brian Robinson, Anuradha Rao, and Paul Dawson acquired data; Courtney Ferrebee, Jianing Li, Jamie Haywood, Anuradha Rao, Brian Robinson, Rheinalt Jones, Benjamin Hinrichs, and Paul Dawson were responsible for the analysis and interpretation of data; Courtney Ferrebee, Rheinalt Jones, and Paul Dawson drafted the manuscript; Rheinalt Jones and Paul Dawson obtained funding; and Paul Dawson was responsible for study supervision.

Conflicts of interest

The authors disclose no conflicts.

Funding

This research was funded by the National Institutes of Health, National Institute of Diabetes and Digestive and Kidney Diseases grants DK047987 (P.D.) and DK098391 (R.J.), the Emory University Integrated Cellular Imaging Microscopy Core of the Emory+Children's Pediatric Research Center and Children's Healthcare of Atlanta and Emory University's Pediatric Biomarkers Core. Also supported by a Research Training in Translational Gastroenterology and Hepatology Training grant (National Institutes of Health T32 DK108735 to B.S.R.), and by a Research Supplement to Promote Diversity in Health Related Research from the National Institutes of Health (DK047987S1 to C.B.F.).